Chemistry in New Zealand

ISSN 2624-1161 (online)

Volume 86, No.2, April 2022

Beyond the academic

Bob Grubbs: Nobel Laureate, & all-round good sort

- Celebrating our regional success stories
- The versatility of sugar in chemistry education
- Towards more energy efficient synthesis of ammonia

Published on behalf of the New Zealand Institute of Chemistry in January, April, July and October.

The New Zealand Institute of Chemistry Incorporated

PO Box 33124
Barrington
Christchurch 8244

Email: nzic.office@gmail.com

Editor

Dr Catherine Nicholson
C/- BRANZ, Private Bag 50 908
Porirua 5240

Phone: 04 238 1329
Email: catherine.nicholson@branz.co.nz

Publishing designer

Natalie Bould
Email: gnatnz@yahoo.com

Advertising Sales

Email: nzic.office@gmail.com

Printed by Graphic Press

Disclaimer

The views and opinions expressed in Chemistry in New Zealand are those of the individual authors and are not necessarily those of the publisher, the Editorial Board or the New Zealand Institute of Chemistry. Whilst the publisher has taken every precaution to ensure the total accuracy of material contained in Chemistry in New Zealand, no responsibility for errors or omissions will be accepted.

Copyright

The contents of Chemistry in New Zealand are subject to copyright and must not be reproduced in any form, wholly or in part, without the permission of the Publisher and the Editorial Board.

Chemistry in New Zealand

Volume 86, No.2, APRIL 2022

Articles and features

Other columns

Comment from the President

Kia ora koutou

Pleasant greetings to you all. I hope this second edition of CiNZ for the year finds you fit and well for 2022. By the time this edition is published, we will be well into the New Zealand government's third stage of its Omicron management plan. COVID-19 community cases have already sharply increased and many educational institutions and businesses could see themselves short staffed due to the need for affected individuals to stay at home if sick.

Already staff at some universities, such as Auckland, have opted to teach online with staff working from home. Other universities have taken a more blended approach. Whatever the case, it is a matter of now living with Omicron or its variants in the community. It's been another quiet period on the NZIC front but events have still been happening in the background and overseas.

At our February Council meeting, it was exciting to preview a new look NZIC website designed by Brendon Gill, a Waikato-based NZIC member from Fonterra. There was seen to be a need for adopting a more "future proofed" website because the current website was built with an older version of Wordpress which will present difficulties with updating. There will be new functionality in terms of messages to individual members and the ability to better control information specific to members. Content from the old webpage will be migrated over to the new site.

It is also anticipated that school memberships will be better managed so that teachers with an email address can create their own teacher accounts free of charge within the environment of a paid school membership. We hope to have this new website later in the year.

There has also been discussion on how we can better support our early career researchers (ECRs) in chemistry by introducing another prize for them to apply for in recognition of their talents. This is in addition to the Easterfield Award, which is often hotly contested due to the high number of excellent applications received. The difficulties noted about the Easterfield award by ECRs are that the timeframes regarding eligibility are restrictive and that often applicants who may be unsuccessful in one round are ineligible by the next round.

It was thought we can introduce a prize in alternate years to the Easterfield Award. As it turns out, there was a proposal from ACES (Asian Chemical Editorial Society) about the introduction of an Early Career Award which we could run every year so amplifying the opportunities for ECRs to apply for awards. This will not only provide an additional option to Easterfield but fill in for it when the Easterfield is not offered. The award is funded by ACES and also promotes publishing within their journals. As a reminder, we as a chemical society are paid royalties if we have New Zealand-based researchers publishing in ACES journals - hence it is a win-win situation. We thank Dr Jack Chen and Professor Paul Plieger for contributions they have made to discussion in this area. Please watch this space as we hope to begin offering this opportunity in 2022.

"As a reminder, we as a chemical society are paid royalties if we have New Zealand-based researchers publishing in ACES journals - hence it is a win-win situation."

In overseas news, Professor Evan Bieske the from University of Melbourne, Parkville, has been appointed to the Editorial Board of the journal Physical Chemistry Chemical Physics (PCCP) and it is good that there is now finally some Southern Hemisphere representation on the Editorial Board. It should be noted that just like the ACES journals, we as a chemical society are also paid if New Zealand-based chemists publish in PCCP.

The amount we received last year amounted to about $1000 so this is definitely something to keep in mind when

Continued

thinking about where to publish research. On the Commonwealth Chemistry front, elections for a new President and Executive Board are afoot we can expect an update on this in due course.

We were asked by the Royal Society of Chemistry (RSC) to lend our support in the form of providing a logo for their "Royal Society of Chemistry Declaration on Pollution". It is recognised that chemical pollution poses an urgent and critical issue for the global community to the extent of being equivalent in importance to biodiversity loss and climate change.

The RSC and other organisations support the creation of a United Nations intergovernmental panel on chemicals and waste management. If this were to be created it would provide for an independent forum that would enable good global coordination and science-informed action on the issue of chemical pollution, potentially saving millions of lives. The New Zealand Institute of Chemistry has agreed to lend support to this call and we have allowed use of our logo in support.

With Pacifichem now past, a reminder that the RACI Chemical Congress will be taking place 3-8 July 2022 at the Brisbane Convention and Exhibition Centre in Brisbane, Australia. The theme for the 2022 National Congress is "Chemistry: Catalysing solutions to global challenges". Please note also that our own national (NZIC) conference will be taking place from 21-24 November 2022 at the University of Auckland and the organising committee has been busy with putting together the details and programme of the conference. We hope for an excellent turnout.

"It is good that there is now finally some Southern Hemisphere representation on the Editorial Board."

Another item discussed at our last Council meeting was ways of encouraging and retaining membership. COVID-19 and the quiet period we have been having has had an impact on membership. We have noted that for student members there is often a big jump in expense in going from a student member to a full-fledged member. To ease this, it was decided that we bring in a "graduate membership" category, where the subscription rate (to be finalised) will be something in the vicinity of $90.00 per year or $160.00 for two years. Once again, watch this space as we bring this in.

As a final word, I will need to start thinking about visiting the branches as is customary in my role. However, Omicron has put this in doubt, at least for the first half of this year. Hence, this may be something I will need to revisit in the second half of the year. I hope that this may be possible so I can come and visit the branches.

Take care everyone.

Noho ora mai

Michael Mucalo, NZIC President

NEWS

AUCKLAND

University of Auckland

STAFF SUCCESSES

Senior Lecturer Davide Mercadante and his colleagues recently published a paper in *Nature Chemistry* explaining how the very strongly bound complex between a histone and DNA might be able to dissociate on biologically relevant timescales [Heidarsson, P.O.; Mercadante, D.; Sottini, A. *et al.* Release of linker histone from the nucleosome driven by polyelectrolyte competition with a disordered protein. *Nature Chemistry* 2022, *14*, 224–231. https://doi.org/10.1038/s41557-021-00839-3]. The paper integrates computational simulations of the disordered proteins with experimental observations.

The University of Auckland published a press release about this work entitled, "Fuzzy molecular threesome is basis of gene expression", which can be found at:

https://www.auckland.ac.nz/en/news/2022/01/11/gene-expression.html

The research was featured in several mainstream scientific news outlets such as Science Daily, Phys.Org, and EurekAlert. The article has generated considerable international interest, currently placing itself in the 97th percentile (ranked 10,227th) of the 399,022 tracked articles of a similar age in all journals and the 85th percentile (ranked 10th) of the 69 tracked articles of a similar age in *Nature Chemistry.*

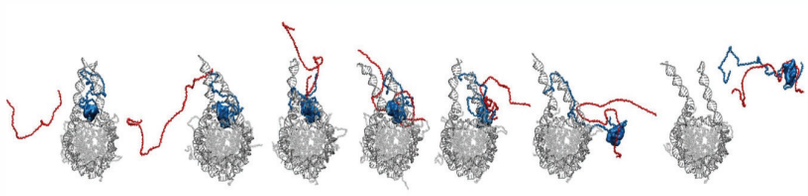

Illustration from Davide Mercadante's publication in *Nature Chemistry.*

Congratulations to the Food Science Programme! The University of Auckland has emerged as the best University in New Zealand in the Food Science & Technology subject area in the recent US News ranking.

Geoff Waterhouse was awarded a Research Excellence Medal for his research on sustainable chemistry, energy, and nanotechnology at the university virtual "Celebrating Research" event.

Ralph Cooney was made an Officer of the New Zealand Order of Merit for services to science and innovation in the New Year Honours. The citation noted that Ralph has led development of significant innovative national research and development networks between researchers and companies in New Zealand to assist transforming the country's economy. Ralph has had a significant impact on the School of Chemical Sciences in addition to being Head. The postgraduate programmes in Food, Forensic Science, Polymers and Wine Science all resulted from his leadership and contacts outside the University.

Associate Professor SallyAnn Harbison MNZM has been appointed to a part-time role as the Director of the Forensic Science Programme for the next year. SallyAnn is a Senior Science Leader in the Forensics section of ESR Ltd, and has been an honorary lecturer with our Forensic Science programme since its inception in 1996. She is an expert in forensic biology, and most recently set up the capability for the Auckland ESR site to conduct genomic sequencing of SARS-CoV-2, the virus that causes COVID-19.

Dr Davide Mercadante has been appointed Director of the Scholar Programmes of The University of Auckland. Davide will undertake tasks involving the organisation and structuring of the programmes, which include a pioneering Science Scholar Programme aiming at training scientists holding both multi-disciplinary and trans-disciplinary skills, and the Bachelor of Advanced Science - a programme aiming to providing students with profiles that delve deeper into research-informed teaching.

STUDENT SUCCESSES

PhD Completions

Qing Wang successfully defended her PhD thesis, "Porphyrin-like iron single atom catalysts on N-doped carbons for the oxygen reduction reaction". Qing was supervised by Geoff Waterhouse, Dongxiao Sun-Waterhouse, Shane Telfer (Massey) and Tierui Zhang (Chinese Academy of Sciences).

Auckland University of Technology

NEW FACES

Dóra Laczi joins the chemistry department for a PhD under the supervision of Dr Cassandra Fleming. Dóra's research focusses on the development of light-responsive drug transport systems that deliver drugs selectively to specific sub-cellular compartments.

CONGRATULATIONS

A huge congratulations to Dr Cassandra Fleming, who was announced as the AUT Emerging Researcher at the AUT Excellence Awards on the 10th of February for her work on photoresponsive caging groups for biomedical applications.

Dr Jack Chen was awarded SfTI Impact acceleration funding for the project, "Cellulose-based surfactants". Jack's team will be developing sustainably-produced surfactants for applications in industry as emulsifiers, wetting agents and solubilisers.

Professor Nicola Brasch, her former PhD student, Dr Vinay Bharadwaj, and collaborators in the US published an article in *The Journal of Organic Chemistry* entitled, "Exploring the potential of 2-(2-nitrophenyl) ethyl-caged *N*-hydroxysulfonamides for the photoactivated release of nitroxyl (HNO)".

Dr Jack Chen and Dr Cassandra Fleming's book chapter on "Seven-membered rings" is now online as part of the book series, "Progress in Heterocyclic Chemistry", published by Elselvier.

CANTERBURY

University of Canterbury

PRIZE WINNERS FOR 2021

Congratulations to the following recipients of the Chemistry prizes:

NZ Institute of Chemistry Prize:	Finlay Player
Haydon Prize – Chemistry:	Daniel Chong and Diana Sosnovskaya
Ralph H Earle Jnr Seminar Prize:	Joel Schuurman
CE Fenwick Prizes in Chemistry:	AlexisBlackie
C E Fenwick Prizes in Chemistry:	Thomas Watson and Sydnee K oia
Cuth J Wilkins Prize:	Hilde Martens
Jack Fergusson Prize:	Lachlan Smith

POSTGRADUATE STUDENT RESEARCH SHOWCASE 2021

The School of Physical and Chemical Sciences held its 2021 Postgraduate Showcase afternoon on 25 November 2021. This was an all-day event that celebrated the research endeavours of our MSc and PhD postgraduate students. There were 20 presentations over three sessions, followed by a fantastic plenary seminar by Dr Anna Garden (University of Otago). At the conclusion of the Showcase, the judges (Associate Professor Deb Crittenden, Associate Professor Chris Fitchett and Associate Professor Sarah Masters) had the tough decision of determining our prize winners:

The prize for best Master's presentation went to Hayden Masterton (Gaw research group), for his presentation entitled, "Plastics as vectors for metals in the marine environment", sponsored by RSC-NZ.

The prize for best 1st year PhD presentation went to Brooke Matthews (Kruger research group), for her presentation entitled, "Hoffman-like hybrid ultramicroporous materials for selective gas adsorption", sponsored by NZIC.

The prize for best 2nd year PhD presentation (Ralph H. Earle Jr Seminar Prize) went to Joel Schuurman (Brooksby research group) for his presentation entitled, "Modifying perovskite electrodes for solar cells". This prize was bequeathed to the School by the late Ralph H. Earle Jr., who strongly believed that chemists should appreciate the importance of being able to verbally communicate their subject.

Finally, our prize for best 3rd year PhD presentation went to Max Caplin (Foley research group), for his presentation entitled, "Synthesis of topologically complex fragments for drug discovery", sponsored by RSC-NZ.

Overall, it was brilliant to see the vibrant diversity of research ongoing in the school, and the quality of the presentations was excellent.

PHD COMPLETIONS

Xin Qiu was supervised by Professor Antony Fairbanks. Xin's thesis was titled, "New protecting group free transformations of carbohydrates". The viva voce exam took place over Zoom and Xin was examined by Professor David Larsen (Otago).

Shailendra Sharma was supervised by Vladimir Golovko and Aaron Marshall (CAPE). The title of his thesis was, "Synthesis and activation of metal cluster-based electrocatalysts for CO_2 reduction".

Nic Bason was supervised by Chris Fitchett. Nic's thesis was titled, "Oligo-aryl acenes and oxidative cyclodehydrogenation". The viva voce exam was conducted by Associate Professor Nigel Lucas (Otago) with Professor Jonathan White (Melbourne) as the external examiner.

PROFESSOR IAN SHAW IN THE NEWS

Professor Ian Shaw was interviewed for the Stuff article, "Council continues use of controversial weedkiller, but risk to public deemed 'low'" (by Jonathan Guildford, posted Jan 8, 2022). He said in reference to the commonly used herbicide, glyphosate, that the amount being sprayed in Ōtautahi Christchurch appears to be quite low and wouldn't pose much risk to the public, but we should reduce our use of the herbicide anyway. This informative article including Ian's comments can be found at:

https://www.stuff.co.nz/environment/127352302/council-continues-use-of-controversial-weedkiller-but-risk-to-public-deemed-low

MANAWATU

The Manawatu branch of the NZIC hosted a Global Women's Breakfast at Café Cuba on 16 February, with eleven people in attendance. This was one of over 400 breakfasts held worldwide as part of a global event to celebrate women in chemical science and engineering. We were grateful to our guest speaker, Dr Jingjing Wang, who spoke about balancing her role as a senior chemist at New Zealand Pharmaceuticals with being a mother to young Meilan.

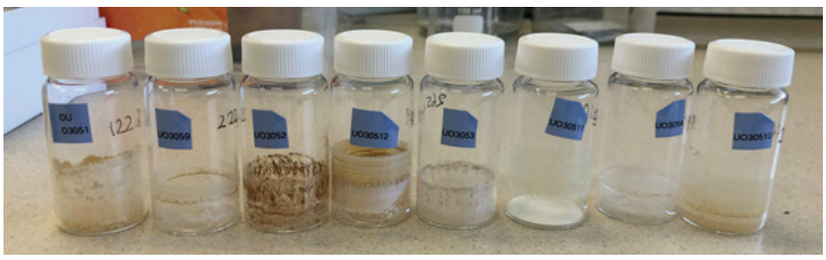

Sample vials of novel benzoxazole amides, synthesised by CHEM 305 students as part of the Drugs for Neglected Diseases initiative (DNDi) Open Synthesis Network

OTAGO

University of Otago, Department of Chemistry

Third-year CHEM 305 Biological Chemistry students undertake a laboratory associated with the Drugs for Neglected Diseases initiative (DNDi) Open Synthesis Network. The project undertaken in 2021 was published in the Journal of Chemical Education (DOI: 10.1021/acs.jchemed.1c01213), with undergraduate students, lab demonstrators and various other academic staff as authors and Dr Ben Perry (DNDi) and Dr Andrea Vernall as corresponding authors.

CHEM 305 students undertook the synthesis, purification and chemical characterisation of a series of novel benzoxazole amides, which were compounds of interest against Leishmania donovani to treat visceral leishmaniasis. The novel compounds were then tested by DNDi's collaborators and revealed several interesting activities (for more information, refer to the paper).

An Open Synthesis Network project is something we hope to continue year-on-year in CHEM 305.

Summer students Alyssa Mohd Sukri, Elouan Hay-Fourmond, and Meg Threlfall (Christina McGraw's lab) joined the December Munida Time Series Research Cruise. This bimonthly NIWA/Otago transect is the longest running marine climate change time series in the Southern Hemisphere.

In late 2021, Professor Sally Brooker and Michael Bennington teamed up with Dr Dave Warren and Outreach team members Samantha McIntyre and Vachrisa Stevenson, plus Hamish Tonkin (GWD motor group; Hyundai Nexo hydrogen fuel cell car) and MC Ra Dallas (Nga Kete Matauranga Pounamu Charitable Trust, for Murihiku Regeneration), for a series of seven Invercargill school visits plus a visit to SIT, focussed on green hydrogen.

Sally was thrilled to get the opportunity to drive the Nexo!

Sally Brooker driving the Nexo! (Outreach team photo credit: Brenda Goodwill at Southland Girls High).

Sally is particularly proud of her recent PhD graduates who have managed to complete their degrees during the pandemic despite the additional stress of being separated from their families overseas during these uncertain and challenging years.

One of these graduates, Dr Sandhya Singh, who turned down a JSPS fellowship due to the Japanese border being closed, has instead taken up a postdoctoral fellowship with Professor Sophie Beeren at DTU, Denmark, working on enzyme-mediated dynamic combinatorial chemistry.

Another of Sally's team, Sriram Sundaresan, has also started a research fellowship, in this case with Professor Eva Rentschler at Mainz University, Germany. He is working on single molecule magnets, and will co-supervise some spin crossover masters candidates.

The group of Anna Garden welcomes new students in 2022. Chris Mills and Nicholas Smith are returning to the group as PhD students after their successful Honours study. Elouan Hay-Fourmond joins the group as a BSc (Hons) student.

Nick and Elouan are working on method development for nanoparticle structural elucidation and Chris will be studying catalytic surfaces for battery technology.

Nicholas Smith was awarded the P. K. Grant prize for the Honours student who best demonstrates excellence in experimental skill and research methodology. Congratulations, Nick!

Congratulations to first class BSc (Hons) graduate Varinder Singh who has been offered an Otago University PhD scholarship and started work in Sally's team on developing and testing CO2 reduction catalysts on 1 March. He has also just had his first paper accepted, on an HER catalyst he made, characterised and tested during his CHEM390 project and completed over the subsequent summer *(Dalton Trans. 2022, DOI*

Green hydrogen school visits in Invercargill. (L to R) Hamish Tonkin, Sally Brooker, Ra Dallas, Samantha McIntyre, Vachrisa Stevenson, Michael Bennington, Dave Warren.

Left, Dr Sandhya Singh in Copenhagen after taking up a postdoctoral fellowship at DTU.

Below, Sriram Sundaresan (left) with Professor Eva Rentschler and the rest of her research group, Mainz, Germany.

10.1039/D2DT00141A). Hajie Tamorite is also joining Brooker's Bunch in 2022, to do his PGDipSci.

Congratulations to Dr Rosa Diego Creixenti on completing her PhD defence at the University of Barcelona. It was a pleasure to have hosted her in Brookers Bunch from January to July 2020, albeit this was a more 'interesting' experience for her than expected, due to the sudden appearance of COVID-19!

WAIKATO

University of Waikato

Congratulations to the 2021 winner of the Waikato Branch's JE Allan Memorial Prize for the top second year chemistry student, Keeley Reiher.

Congratulations also to Aphiwat Kaewthong (Golf) who has completed his PhD with Bill Henderson on, "Investigation of the coordination chemistry of thiosulfate ligand via an ESI-MS directed synthesis strategy", and also to Simeon Atiga and Sam Murray on submission of their PhD theses.

Atiga worked with Bill Henderson on the coordination chemistry of analogues of the thiosalicylate ligand and Sam worked with Michèle Prinsep (and other supervisors, Tim Harwood and Jonathan Puddick at Cawthron) on characterisation of cyclic sulphated polyethers produced by toxic Gambierdiscus species.

Amber Bell has successfully submitted her MSc thesis titled, "An investigation of low diastase activity in manuka honey" and is starting her PhD, investigating the effect of heavy metals on bees with Megan Grainger. This work is part of Megan's Faststart Marsden project.

Jade te Bogt is starting her MSc, investigating the optimisation of oil infusion technology, also with Megan Grainger and in collaboration with Analytica laboratories and Whio Innovations.

Above, Brooker's Bunch group members 2022 (left to right) Michael Bennington, Hajie Tamorite, Varinder Singh, Matt Robb

Left, Former Brooker Bunch visiting researcher Dr Rosa Diego Creixenti with her recently completed thesis

Megan Grainger with some busy bees!

As part of the IUPAC Global Women's Breakfast event on 16 February for female chemists and supporters, a very enjoyable breakfast was held at Jack's Coffee Lounge in Hamilton. This was one of nearly 400 events held in over 70 countries. Given the time differences, we were also the very first breakfast to launch.

Megan Grainger featured on Radio New Zealand's podcast "Our Changing World", talking about her honey research and has found that honeys from different regions in the North Island have elemental fingerprints that can help to categorise them into areas of origin. She also found traces of heavy metals in the honey and is investigating the impact of these on bee activity and determining the extent to which they might lead to declining bee populations and colony health.

Michèle Prinsep was an invited keynote speaker at Pacifichem 2021 in the symposium, "The science of marine natural products: towards understanding of the physiology and ecology of marine life". She gave a talk entitled, "Chemical ecology of some Australasian nudibranchs."

WELLINGTON

The Wellington Branch AGM took place in December 2021, at which Professor Martyn Coles was presented with the 2022 Maurice Wilkins Centre Prize for Chemical Science – congratulations! This was followed by a beautifully illustrated talk by Professor Tricia Hunt on "Hydrogen bonding in ionic liquids".

WAIKATO NZIC BRANCH COMMITTEE

The Waikato NZIC branch committee for 2022 is as follows:

Chairperson:	Bill Henderson
Secretary:	Brendan Gill
Treasurer/Chemistry Education representative:	Martina Pietsch Brown
Council delegate/Branch editor:	Michèle Prinsep
Student representatives:	Amber Bell and Shaun McNeil
Committee members:	Megan Grainger, Lauren Gris, Michael Mucalo, Nikki Webb

Martyn Coles receiving the Maurice Wilkins Centre Prize from Wellington Branch Chair Nate Davis (Photo credit: Joanne Harvey)

Chemistry Teachers' Day

The annual Chemistry Teachers' Day hosted by the School of Chemical and Physical Sciences was held on 2 December 2021. Fifty high school teachers from the Wellington and Nelson region joined us for a day of guest speakers, discussion groups, workshops and lab activities.

The day was kick started with some fascinating talks from Dr Helen Woolner and Associate Professor Franck Natali about their current research. This was followed by an engaging discussion from student alumni who talked about where a degree in chemistry had taken them, followed by a seminar from Professor Justin Hodgkiss who highlighted the links between a chemistry degree and the emerging tech industry within Aotearoa.

The day ended with a scholarship workshop led by Dr Suzanne Boniface and lab demonstrations led by Dr Courtney Davy. It was a great opportunity for the teachers to come together for networking, to discuss teaching practices, NCEA standards, university entrance and gain insights into the latest developments in chemistry research within our School.

Participants in the Chemistry Teachers' Day (Photo credit: Courtney Davy)

VUW

Dr Shalini Divya, who is the co-founder and CEO of the New Zealand start-up TasmanIon, received the "KiwiNet Breakthrough Innovator Award" in the 2021 KiwiNet Research Commercialisation Awards in November 2021.

This award "recognises an upcoming entrepreneurial researcher who is making outstanding contributions to business innovation or is creating innovative businesses in New Zealand through technology licencing, start-up creation or by providing expertise to support business innovation".

STUDENT SUCCESSES

Congratulations to VUW students who have recently successfully completed their PhD examinations.

Aleksandra (Sasha) Ilina, Anindita Sen and Isabella Wagner – all from Professor Justin Hodgkiss' group – defended their theses titled, "Ultrafast dynamics of the eumelanin pigment", "Colorimetric aptasensors for the detection of methamphetamine in saliva" and "An ultrafast spectroscopy study of excited state dynamics in perovskite semiconductors for optoelectronic applications" respectively.

Ethan Woolly (supervised by Associate Professor Paul Teesdale-Spittle and Associate Professor Joanne Harvey also defended his thesis titled, "Designing new agents for the peloruside binding site".

Wellington Branch held a virtual get-together on 16 for the IUPAC Global Women's Breakfast. Networking and engaging discussions about gender equity in science were complemented by videos of Drs Shalini Divya and Emma Wrigglesworth featuring their roles in successful New Zealand chemistry start-up companies.

Dynamic science

The School of Chemical and Physical Sciences (SCPS) held a two-day event in January called "Dynamic Science Wellington" for high school students in Years 12 and 13 who are passionate about chemistry and physics.

The first day included a series of engaging activities in the research labs where the students gained hands-on experience and insight into cutting-edge research within SCPS.

The second day started with a trip to the Robinson and Ferrier Research Institutes where the students learned about the connection between SCPS and industry.

They gained an understanding of how chemistry and physics can contribute to New Zealand's scientific community, allowing them to see where a degree in chemistry and physics can take them.

The day ended with a fun and challenging chemistry and physics escape room, where the students had to use the knowledge they gained throughout the past two days to solve puzzles and clues in order to break out of the lab.

Dynamic Science Wellington was a successful event that inspired the students and got them excited to further their studies in chemistry and physics.

Obituary

Robert H. Grubbs

Nobel Laureate, 1942-2021

On the morning of 21 December 2021, I completed a four-day tramping trip with three friends on the Ella Range tops of Nelson Lakes National Park. On our way back to Christchurch, we visited a café in Murchison where I checked my cell phone to catch up on the world's happenings. My attention was immediately drawn to a text message from friend and chemistry academic colleague, Antony (Fez) Fairbanks: "Very, very bad news I'm afraid … Bob Grubbs has died."

Bob Grubbs was a US academic research chemist of immense international standing; it is easy to find details of his heralded career and achievements on the internet. It is not my intention in this article to reiterate those details, but it is probably worth sketching a few points to set the scene for my purpose.

Robert Howard Grubbs was born on February 27, 1942, on a farm near the evocatively named town of Possum Trot, Kentucky. After his father's return from WWII service, his family moved to Paducah, Kentucky, where Bob attended Paducah Tildman High School. He subsequently studied at the University of Florida, completing a BS in chemistry in 1963 and MS (with Merle Battiste) in 1965, before undertaking a PhD (1968) researching organometallic compounds with Ronald Breslow at Columbia University. During his time at Columbia, Bob met Helen O'Kane, a special-education teacher; they were later married and had three children: Barney (born 1972), Brendan (1974) and Kathleen (1977).

Bob Grubbs with Ernest Rutherford's 1908 Nobel Prize Medal in Chemistry

In the period 1968-69, Bob held an NIH Fellowship at Stanford University conducting early research on organometallic catalysis. In 1969, he was appointed Assistant Professor at Michigan State University, where he began work on olefin metathesis. He was promoted to Associate Professor in 1973, then moved to California Institute of Technology as Professor in 1978. From 1990 he was the Victor and Elizabeth Atkins Professor of Chemistry at Caltech. During his research career, he was the recipient of many honours, awards and prizes, most notably the 2005 Nobel Prize in Chemistry.

Bob was demonstrably a great scientist – but equally demonstrably (though perhaps less generally well known), he was a wonderful all-round person. He was also very tall – well over six feet (in non-S.I. units). Bob and Helen visited New Zealand on three occasions and became great friends of members of the University of Canterbury (UC) chemistry community. In this missive, I mean to tell the story of my perception of Bob Grubbs beyond the chemistry, relating some of the non-academic experiences that I, my life partner Wendy and our friends enjoyed with Bob and Helen.

Above: Bob Grubbs and his host, Richard Hartshorn, prior to delivery of Bob's Prestige Research Seminar just hours after the announcement of the 2005 Nobel Prize in Chemistry.

Left: Noble Prize celebration party, 7 October 2005. Left to right, Peter Steel, Bob Grubbs and Martin Banwell.

The University of Canterbury (UC) has an academic visitors' programme called the Erskine Fellowship, named after a contemporary of Ernest Rutherford, Jack Erskine, who endowed the funds that support the programme. One of the aims of the Erskine Fellowship is to attract eminent researchers and teachers to visit the UC for the benefit of its students. For the year 2005, Richard Hartshorn, an academic member of the Department of Chemistry, nominated Professor Robert H. Grubbs, whom Richard had met during his postdoc at Caltech. Somewhat presciently, the nomination said in part: "Several staff have commented that his academic stature and the quality of his research make him a very strong candidate for the Nobel Prize in Chemistry." At that time, I was Head of the Department (HoD) of Chemistry, so had the formal responsibility of offering Bob (whom I had never previously met) a Fellowship. I was pleasantly surprised that he accepted it almost immediately.

Bob and Helen's visit to UC turned out to be a wonderful event, one of highlights of my time as HoD. Bob was not only a superb research chemist, but also wonderful teacher of students at both undergraduate and postgraduate levels. Although most of them were (at that time) unaware of his eminence, the students loved Bob's lecturing style and approachability. But it was not just the chemistry that made Bob and Helen's visit so special. They were affable and convivial, involving themselves enthusiastically in the department's social activities. Through those activities I learned that we shared several extra-curricular interests, most particularly a love of the outdoors [Bob was an enthusiastic and proficient hiker/tramper, rock climber, canyoner and fisherman and the cover of J. Polymer Sci. A, 55 (18), 2017 features a picture of Bob and Chris Bennen on the summit of the Eichorn Pinnacle in Yosemite National Park, CA]. So Bob and I agreed that we should undertake a tramping trip in the mountains before he completed his visit.

In the first week of October 2005, Bob and Helen visited the North Island where Bob presented seminars at several universities. They returned to Christchurch on Thursday 6 October (New Zealand time) because Bob was scheduled to deliver an undergraduate lecture the next morning. That evening it was announced

that, along with Yves Chauvin and Robert Schrock, Bob had been awarded the 2005 Nobel Prize for Chemistry. I heard the news on the radio but didn't attempt to contact Bob, knowing that he would be more than busy dealing with undoubted international professional and media interest from around the world. He later told me that, a bit after midnight, he disconnected his phone so that he and Helen could get some sleep.

Early the next morning, Bob came to my (HoD's) office saying that he needed to talk urgently after his lecture. I congratulated him on his award and accompanied him to the lecture theatre (Room 533 of the then Rutherford Building), where the students and the many staff who had spontaneously congregated there, gave him a standing ovation iIn an obituary for Bob in the New York Times of 26 January 2021, an accompanying image is of Bob receiving applause from the students in Room 533 -- Robert H. Grubbs, 79, Dies; His Chemistry Breakthrough Led to a Nobel - The New York Times (nytimes.com)].

Back in my office, post-lecture, Bob explained that he was going to have to fly back to Caltech in a few days to fulfil the expectations and obligations that came with the Nobel Prize announcement. Consequently, he wanted to shift forward his research seminar; and, more importantly, that we must head into the mountains for a tramping trip that weekend!

During that day, Roy Sharpe, UC's then Vice Chancellor, invited Bob to have a photo taken with Ernest Rutherford's original 1908 Nobel Prize medal in Chemistry. Later in the afternoon, Bob gave a hurriedly rescheduled Prestige Research Seminar to a packed audience in UC's largest lecture theatre. During the afternoon, Wendy (especially) and I organised a celebratory party that was held at our home that evening and attended by many of the people that Helen and Bob had got to know during their stay, along with several

2005 Nobel Prize celebration party: Helen and Bob cut the cake

"It says a lot about Bob that his priority for the morning after the announcement of his Nobel Prize was to fulfil his lecturing commitment to the students – something I am sure that they will always remember."

UC notables including the Chancellor and Vice Chancellor. A few months later, Bob was appointed by the UC Council as the inaugural Honorary Distinguished Professor of the University.

The weather forecast for the next day was wintery, but Bob remained adamant that we must go walking in the mountains. So, next morning, Bob, Wendy and I headed 130 kilometres inland from Christchurch to the settlement of Bealey, where we met academic colleague Rod Claridge and his wife Mary, at their bach. It was snowing when we arrived and continued do so for the couple of hours it took for the five of us to climb about 650 metres over six kilometres to the historic musterers' shelter called Bealey Spur Hut.

While we were at the hut, the snow stopped and the weather improved to the point where the sun came out and it was warm enough to sit outside for lunch. I still cop occasional ribbing from colleagues about "luring" Bob into the winter wilderness

Wendy Williamson, Helen Grubbs and Bob Grubbs at the Godley Head gun emplacements, 16 December 2008

of the South Island mountains before his investiture as a Nobel laureate.

As Bob had expected, he was recalled to Caltech before his Erskine Fellowship had ended. But he told me that he and Helen fully intended to return once the "fuss had died down"; and indeed they did – twice.

The first of those return visits was as a plenary speaker at an Australasian Inorganic Chemistry Conference (IC08) being held at UC in December 2008. During that stay, Bob delivered a research seminar to the UC Faculty of Science and a public lecture marking the centenary of the presentation of the 1908 Nobel Prize in Chemistry to Ernest Rutherford.

On the weekend, Helen, Bob, Wendy and I went for a walk to historical military tunnels, blockhouses and gun emplacements at Godley Head, near the entrance to Lyttelton Harbour. Bob found the site very intriguing and expressed surprise that New Zealand had felt a need for such defences at such a large distance from the centres of the twentieth-century wars. Being as tall as he was, he cracked his head on the roof of a communication tunnel, but continued, unfazed, using a handkerchief to nonchalantly deal with the resultant trickle of blood.

Wendy's and my next encounter with Bob and Helen was in July 2010. After a post-HoD visit to Europe, we returned to New Zealand through the US, taking up Helen and Bob's

At Bealey Spur Hut in snaw on 8 October 2005. Left to right: Wendy Williamson, Bob Grubbs, Rod Claridge and Mary Claridge.

Bob Grubbs presents a research seminar to the University of Canterbury Faculty of Science on 9 December 2008.

invitation to visit them in California. They were consummate and relaxed hosts. Over the first couple of days, Bob showed us around Caltech and other sites in the vicinity of Pasadena. We had barbecue meals, swam in their backyard pool and watched baseball on television with their younger son, Brendan.

On the third day, we packed into their van and drove 430 kilometres to Sequoia National Park, where

we joined some of Bob and Helen's friends, colleagues and students for three days of camping, hiking and sightseeing. Wendy and I learnt about bear-etiquette (we had black bears around our tents at night), and Bob pointed out some of the peaks and rock-faces that he had climbed.

On the second day, Bob invited me on a day of fly-fishing, but, knowing nothing about that art, I preferred to join his students on a 22-kilometre jaunt to Pear Lake, which, at just over 2900 metres, was, at that time, the highest I had ever been above sea level. We didn't have trout for dinner that evening with Bob explaining that his day's activities were called "fishing", not "catching".

Port Hills walking party, 15 September 2011. Left to right: Marie Squire, Bill Swallow, Chris Fitchett, Antony (Fez) Fairbanks, Bob Grubbs, Vladimir Golovko, Wendy Williamson.

Bob and Helen's second return visit to Canterbury, in September/October 2011, was formally another Erskine Fellowship, to compensate for time they had lost in 2005. On the first weekend, a group of chemists and chemistry-associates whom Bob had got to know socially, joined us on a 12.5 kilometre walk along the Port Hills, the volcanic crater rim that separates Christchurch from the Port of Lyttelton. This was seven months after the disasterous Christchurch Earthquake of February 2011, and Bob professed awe and sadness at the extent of the damage that was still evident in the hillside suburbs that we traversed on our descent back to the city.

Although I had now done a fair amount of walking with Bob, each trip had been of only a few hours duration and we were still keen to undertake a more challenging venture of the sort we had envisaged back in 2005. So, we teamed up with UC Chemistry academics Fez Fairbanks and Andy Pratt for the two-day Casey-Binser Track in Arthurs Pass National Park. On Thursday 6 October, the four of us drove to the trailhead and set off up Andrews Stream, across the saddle at Hallelujah Flat and down Casey Stream to Casey Hut – a six-hour journey of 20 kilometres with 700 metres of total ascent.

Bob commented that the hut reminded him of his youthful dwellings in rural Kentucky; and soon after our arrival, he was youthfully swinging an axe, splitting logs for the wood-fired stove.

We were soon comfortably ensconced in the hut with hot drinks and food cooking on the stove [in early October 2015, almost four years to the day after our visit, Casey Hut burnt to the ground, probably due to careless use of the stove].

Bob Grubbs splitting logs at Casey Hut woodshed

About to start on the Casey-Binser Track. Left to right: Antony (Fez) Fairbanks, Bob Grubbs, Andy Pratt and Bryce Williamson.

Bob Grubbs, Fez Fairbanks and Andy Pratt traversing Hallelujah Flat on the Casey-Binser Track

After dinner, we sat around in the warmth of the hut, telling stories and sipping Scotch from coffee mugs.

The next morning, we rose early and headed down the valley of Poulter River for about 14 kilometres over four hours, to Pete Stream, where we ate lunch.

After lunch, we climbed for about 600 metres through native beech forest to Binser Saddle, which, at an altitude of nearly 1100 metres, was still covered in snow. Beyond the saddle, we had a steep 500-metre descent to the Waimakariri River flats, where Andy (who had gone ahead at lunch) met us in the car that he had retrieved from a couple of kilometres further up the road. Over the day, we had covered nearly 23 kilometres with 800 metres of total ascent over just less than seven hours. That was enough, we thought, to adjourn to the University of Canterbury Club for well-deserved Friday-evening beers.

Bob's 2011 Canterbury visit was the last time I saw him. In the intervening years, several colleagues met Bob at conferences, such as Pacifichem, and I was told that he was always eager for news of his many friends, both from the UC Chemistry Department and throughout New Zealand. We kept in touch through occasional email messages where we mentioned families, world news and outdoor activities far more than we ever discussed chemistry.

I am regretful that my last communication to him was a succinct and poorly written email as long ago as May 2020 -- small-talk about tramping in Tasmania, the (early) ramifications of Covid-19 and the state of the University of Canterbury Club's building following post-earthquake repairs. On December 19, 2021, aged 79, Bob died at the City of Hope Comprehensive Cancer Centre in Duarte, CA, where he was being treated for lymphoma. He is survived by Helen, his three children, four grandchildren and two sisters. The world is a lesser place without him.

Okioki i runga i te rangimarie Bob.

Contributed by Bryce E. Williamson, Emeritus Professor, School of Physical and Chemical Sciences | Te Kura Matū University of Canterbury | Te Whare Wananga o Waitaha

With thanks to Wendy Williamson, Richard Hartshorn and Antony (Fez) Fairbanks for jogging my memory and improving my prose.

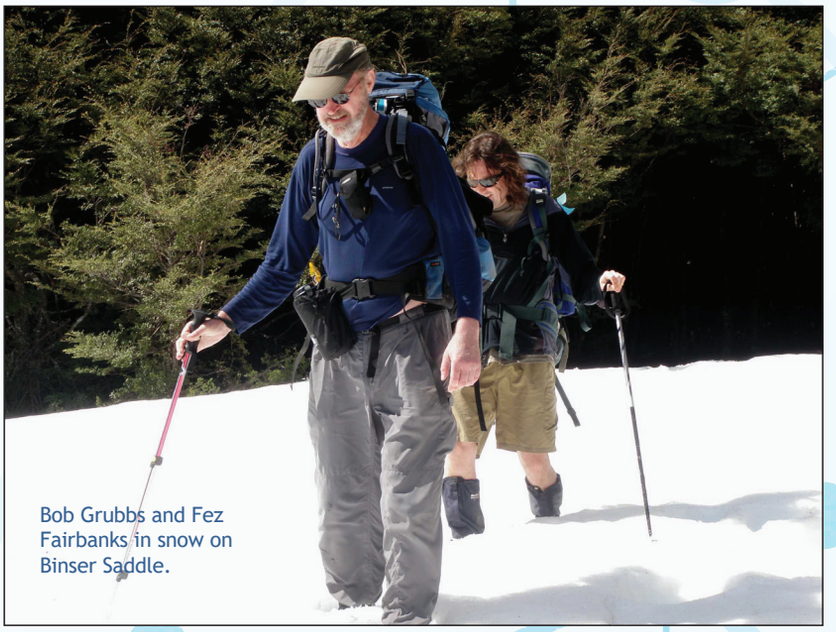

Bob Grubbs and Fez Fairbanks in snow on Binser Saddle.

Article

Mössbauer spectroscopy for distinguishing μ3-OH versus μ3-O bridging in heptanuclear iron clusters

D. NIROSHA T. DE SLIVA,† GUY JAMESON‡ AND TYSON DAIS†*

† School of Natural Sciences, Massey University, Palmerston North and ‡ School of Chemistry and Bio21 Molecular Science and Biotechnology Institute, The University of Melbourne, Australia (Email: t.dais@massey.ac.nz)

Keywords: *transition metal clusters, X-ray crystallography, Mössbauer spectroscopy*

Introduction

Polynuclear iron complexes have raised interest due to their importance in both magnetic[1] and biological materials.[2] Salicylaldoximes and derivatised salicylaldoximes are well known to form multinuclear species, often featuring three-fold symmetric triangular metal rings (Fig. 1).[3]

The study of salicylaldoxime based iron clusters has been fuelled by the presence of analogous Fe_3O triads observed in biologically important metalloproteins[4] and also as analogues of magnetically interesting manganese complexes.[5] The first iron-salicylaldoximato cluster reported was a tetra-iron species, $[Fe_4(saoH)_4(sao)_4]$,[6] of which the chemistry was later extended by Raptopolou et al.[3a] to produce a tri-iron(III) compound with a $[Fe_3O]^{7+}$ core, coordinated by five benzoate ions and a salicylaldoximato di-anion. The hepta-Fe(III) complexes presented here all share the common building block, $[Fe_3O]$, in which Fe(III) are bridged by oximato- and oxo/hydroxo- groups.

There are several examples reported for tri, hexa-, and hepta-iron(III) salicylaldoximato/derivatised salicylaldoximato complexes containing the $[Fe_3O]^{7+/8+}$ core.[5,7] The first polynuclear copper complex with a linked derivatised salicylaldoximato ligand, N,N'-dimethyl-N,N'-hexamethylenebis(5-tert-butyl-2-hydroxy-3-hydroxyiminomethyl) benzylamine (H_4L), was reported by Plieger et al. in 2009.[8] This helical hexa-copper complex provided motivation towards the synthesis of analogous iron(III) compounds with

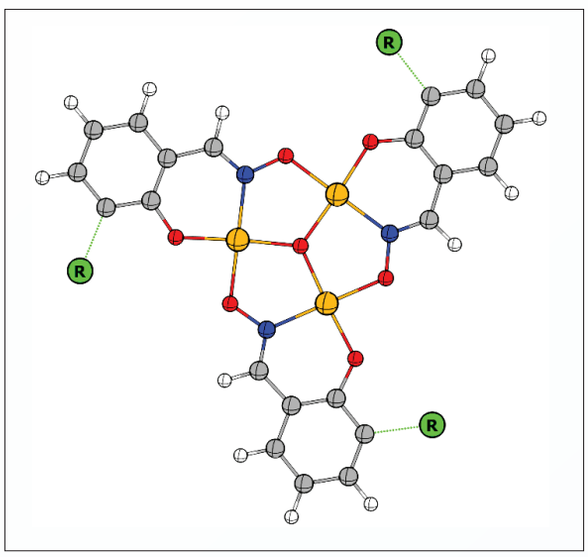

Fig. 1. Schematic representation of the planar $[M_3O(oximato)_3]^{+/++}$ moiety with three-fold symmetry. Metals in gold and R = the rest of the ligand.

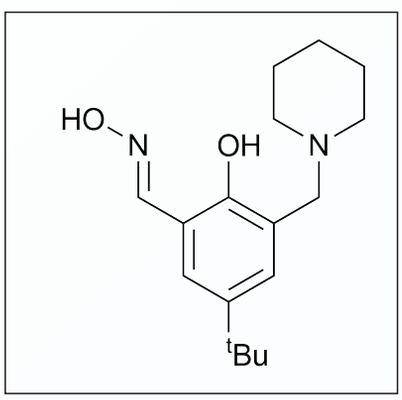

Fig. 2. Chemical structure of the non-linked/single-headed saicylaldoxime ligand, H_2L1, utilised for the synthesis of the Fe_7 complex C1.

the same class of ligands. Herein we report the syntheses and Mössbauer spectra of three new hepta-iron(III) complexes (C1 – C3).

Results and discussion

The first hepta-iron(III) compound, C1, was synthesised using a simple derivatised salicylaldoxime ligand, H_2L1 (2-hydroxy-5-tert-butyl-3-(N-piperidinylmethyl)benzaldehyde oxime) (Fig. 2).[9] Slow evaporation of the filtrate from the 1:1 reaction mixture of $Fe(BF_4)_2 \cdot 6H_2O$ and the ligand in a methanol-pyridine solution led to the formation of dark maroon rhombic shaped crystals of the hepta-iron(III) cluster, $[Fe_7(\mu3\text{-}OH)_2(\mu2\text{-}OH)_6(H2L1\text{-}2H)_5(H2L1\text{-}H)(pyr)_6] \cdot (BF4)_2 \cdot (H2O)_6 \cdot (pyr)_3$ ($C1 \cdot 2BF_4 \cdot 8H2O \cdot 2pyr$) which crystallised in the $R\bar{3}$ space group.

One sixth of the complex C1 represents the asymmetric unit and the full complex is generated by an S_6–$\bar{3}$ improper rotation. There are six molecules of the ligand, H_2L1 in the di-anionic form, $H_2L1\text{-}2H$, in the complex, which are directly connected to six iron atoms (6x μ_3-Fe) that form the two metal triads of $[Fe^{III}_3(\mu_3\text{-}OH)]^{8+}$, which are exactly parallel to each other (Fig. 3). The central oxygen of the triad is formulated as a hydroxo species based on Mössbauer spectroscopy (vide infra).

These triads are linked via six hydroxo

groups that provide the coordination sphere to a seventh iron atom, which sits in the middle of the complex as an anionic unit, $[Fe(\mu_2\text{-}OH)_6]^{3-}$, and is located 3.118 Å from the metal triads (the distance between the metal planes is 6.237 Å).

Each triangle consists of three doubly deprotonated ligands (H_2L1-2H), three iron(III) bound to a μ_3-OH, and three capping pyridine molecules (pyr). Thus, the positive charge (+21) provided by the seven Fe^{III} is overbalanced by -12 from the six ligands, -8 from hydroxo groups [2x(μ_3-OH) + 6x(μ_2-OH)], and -2 from 2xBF_4^- ions present within the lattice. Charge neutrality is achieved by a single proton distributed randomly over the 6 piperidinyl groups of the salicylaldoximato ligand.

A pyridine group and a hydroxo group (μ_2-OH) are axially coordinated to each iron atom with the triangles, resulting in an approximately octahedral geometry. The iron centres of each metal triangle are held together by three N-O groups from the ligands resulting in a bridge between two neighbouring iron atoms where the bridging sequence as Fe-O-N-Fe on both metal triangles.

The central oxygen atom, μ_3-O, of the metal triangle is displaced out of the metal planes by 0.314(6) Å away from the centre of the complex. The consequence is that the axial pyridyl groups tilt slightly away from each other to relieve steric strain. The Fe atom from $[Fe(\mu_2\text{-}OH)_6]^{3-}$ sits in an almost perfect octahedral coordination environment, as a consequence of sitting on the S_6-3 axis. The hour glass-like metallic core of C1 is illustrated in Fig. 3.

Complexes C2 and C3 were prepared in a similar manner to C1 with the use of double-headed derivatised salicylaldoxime ligands H_4L2 and H_4L3, respectively (Fig. 4).

The complexes C2 and C3 are double headed, μ_3-oxo bridged hepta-iron(III) compounds produced in the form of dark red rhombic crystals. Both were obtained in a similar manner to C1, using a 1:2:2 ratio of ligand, $Fe(BF_4)_2{\cdot}6H_2O$, and $NaPF_6$, all in a methanol-pyridine solution. Despite the different amine linkers present in the ligands and the additional non-coordinated species present within the lattices, C2 and C3 are structurally very similar. Each of these clusters contains two approximately parallel oximato- and oxo-bridged metal triangles connected to a central Fe(III) atom via six hydroxo groups.

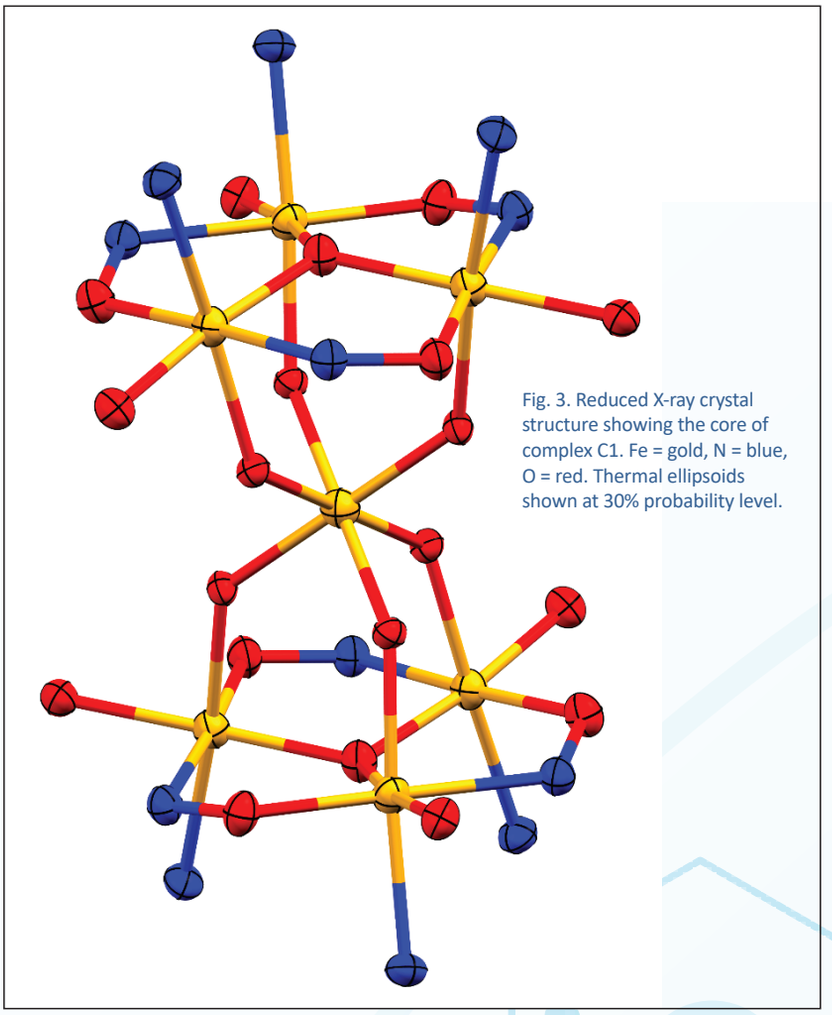

Fig. 3. Reduced X-ray crystal structure showing the core of complex C1. Fe = gold, N = blue, O = red. Thermal ellipsoids shown at 30% probability level.

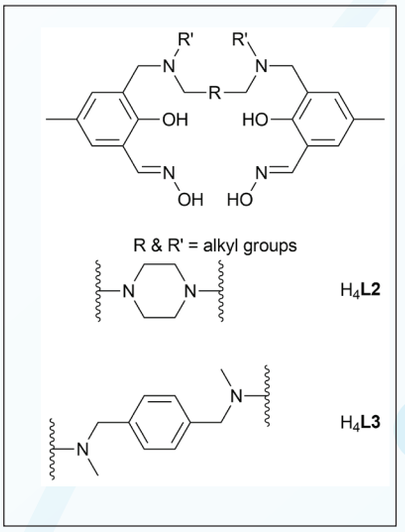

Fig. 4. Structural representation of the linked/double-headed salicylaldoxime ligand (upper) and the diamine linkers of the ligands H_4L2 and H_4L3 (lower)

Of particular note are the Fe-μ_3-oxo bond lengths and displacements of the μ_3-O groups from the Fe_3 planes, which are not significantly different for the $[Fe_3^{III}\text{-}\mu_3\text{-}OH]^{8+}$ moiety of C1. Therefore, there is no crystallographic evidence to distinguish μ_3-O atoms being hydroxo in C1 from oxo

in C2 and C3. In contrast to the $[Fe_3^{III}\text{-}\mu_3\text{-}OH]^{8+}$ of C1, the metal triads are formulated as $[Fe_3^{III}\text{-}\mu_3\text{-}O]^{7+}$ on the basis of Mössbauer spectroscopy. As the ligands utilised for C2 and C3 are flexible linked salicylaldoximes containing salicylaldoxime units on either side, only three ligand molecules are required to form a hepta-iron(III) complex, unlike in C1. Three of these 'salicylaldoxime heads' from three ligand molecules form a lower triangle and the other three 'heads' form an upper triangle (Fig. 1). Due to the flexibility of the di-amine linker between the salicylaldoxime 'heads', these complexes take a twisted helical shape (Fig. 5).

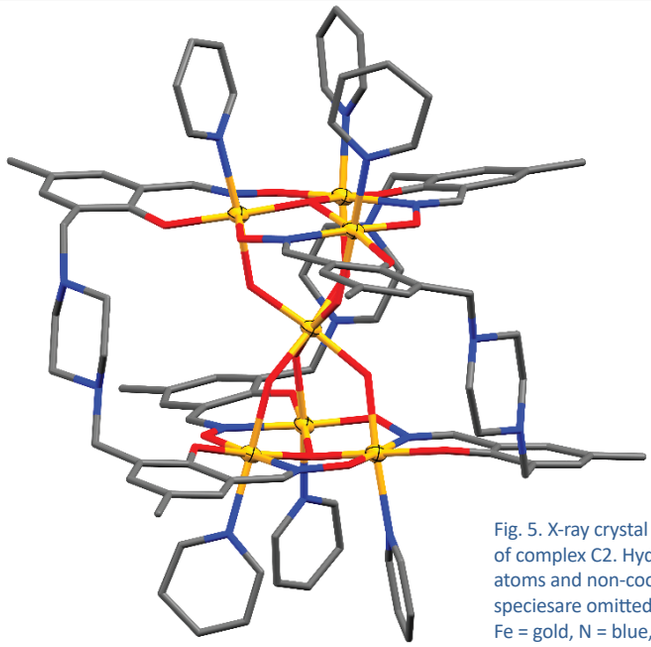

Fig. 5. X-ray crystal structure of complex C2. Hydrogen atoms and non-coordinated speciesare omitted for clarity. Fe = gold, N = blue, O = red. Thermal elipsoids of metals shown at 15% probability level.

Mössbauer spectroscopy

^{57}Fe Mössbauer measurements were performed on complexes C1 – C3 at low and room temperature. Integral fits of the transmission were carried out for the data obtained at room temperature and the parameters for each of the samples are listed in Table 1.

The Mössbauer spectra that were recorded at 293 K illustrate two distinctive fitting lines (red and blue) (Figs. 6 – 8). These two lines can be unambiguously attributed to the two different iron environments present in each complex. The intensity of the blue peaks on the Mössbauer spectra of these complexes is much higher than that of the red peaks. The intensity ratio between the two iron species of each hepta-iron(III) complex was observed to be approximately 7:3, quite close to the expected value of 6:1 as per the crystallographic results, given that the central Fe atom is very tightly constrained relative to the iron triads.

The isomer shift values of these complexes indicate +3 oxidation state and high-spin state of the iron sites[10] and these numbers do not differ significantly among complexes C1 – C3 at 293 K. The quadrupole splitting for C1 (0.50 mm^{-1} and 0.87 mm^{-1}) on the other hand is significantly different

Complex	δ (mm/s)	ΔE_Q (mm/s)	Γ_L (mm/s)	ΓR (mm/s)	I (%)
C1	0.41	0.86	0.37	0.37	77.8
	0.40	0.50	0.21	0.21	28.9
C2	0.40	1.50	0.35	0.35	70
	0.40	0.55	0.35 ± 0.15	0.35 ± 0.15	30
C3	0.40	1.55	0.30	0.30	75
	0.35	0.45	0.35	0.35	26

Table 1. Room temperature ^{57}Fe Mössbauer fitting parameters for C1 – C3 (δ = isomer shift, ΔE_Q = quadrupole splitting, Γ = half height line width, I = intensity)

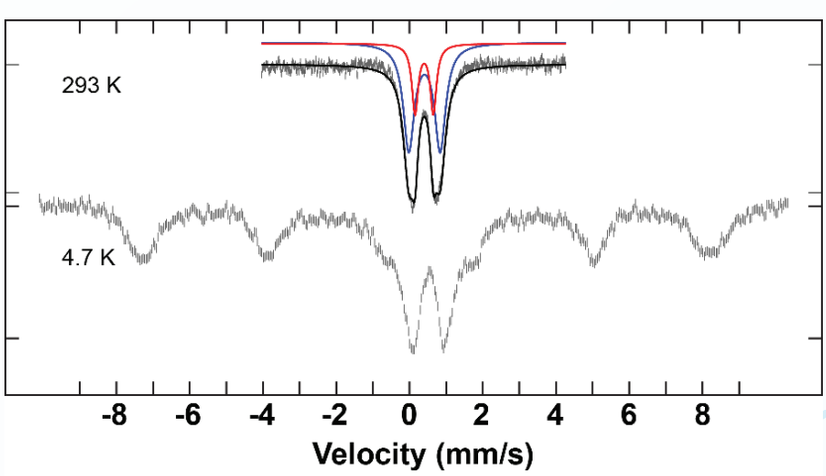

Fig. 6. ^{57}Fe Mössbauer spectra of the complex C1 at high and low temperature, overlaid with corresponding fits using the parameters given in Table 1 at high temperature.

from the values obtained for C2 and C3 (0.45 – 0.55 mm^{-1} and 1.50 – 1.55 mm^{-1}) (see Table 1). The large quadrupole splitting (and relative intensity compared to the other doublet) are consistent with μ_3-oxo groups of C2 and C3. The smaller quadrupole splitting of the doublets of weaker intensity for C2 and C3, and the pair of quadrupole doublets for C1 are consistent with μ_2-hydroxo groups and for C1 the μ_3-hydroxo groups.

Conclusions

Three Fe_7 complexes with structurally similar [Fe_3O – $Fe(OH)_6$ – Fe_3O] type cores have been made, however the exact formulation of the Fe_3O triads contained within each complex could not be determined by X-ray crystallography alone. By comparing the ^{57}Fe Mössbauer spectra, specifically the quadrupole splitting of each complex, it was found that the three iron(III) centres in C1 were linked by a μ_3-OH^- group, as opposed to the μ_3-O^{2-} groups at the centre of each Fe_3 triad in C2 and C3.

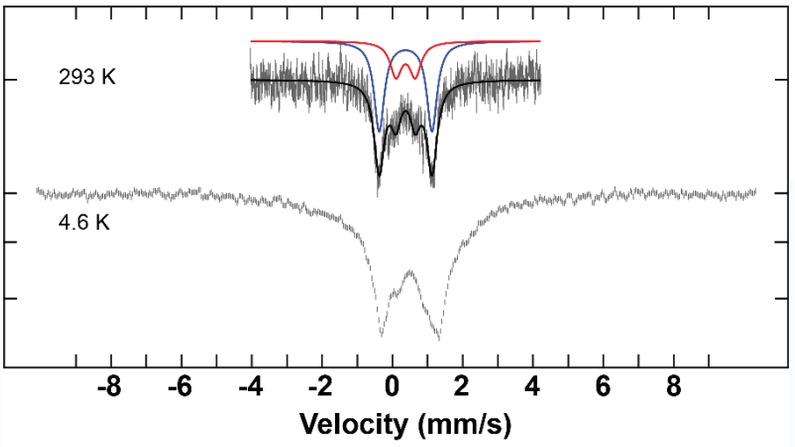

Fig. 7. ^{57}Fe Mössbauer spectra of the complex C2 at high and low temperature, overlaid with corresponding fits using the parameters given in Table 1 at high temperature.

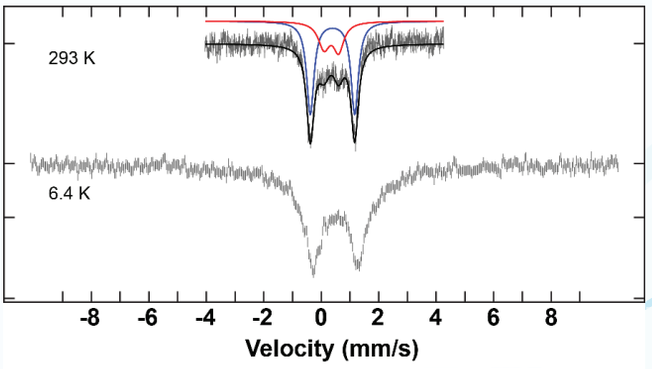

Fig. 8. ^{57}Fe Mössbauer spectra of the complex C3 at high and low temperature, overlaid with corresponding fits using the parameters given in Table 1 at high temperature.

References

1. (a) Vincent, J. B.; Olivier-Lilley, G. L.; Averill, B. A. *Chem. Rev.* **1990,** *90* (8), 1447-67; (b) Cohen, I. A. *Struct. Bonding (Berlin)* **1980,** *40*, 1-37; (c) Horn, A.; Neves, A.; Bortoluzzi, A. J.; Drago, V.; Ortiz, W. A. *Inorg. Chem. Commun.* **2001,** *4* (4), 173-176; (d) Faiella, M.; Andreozzi, C.; Martin de Rosales, R. T.; Pavone, V.; Maglio, O.; Nastri, F.; DeGrado, W. F.; Lombardi, A. *Nat. Chem. Biol.* **2009,** *5* (12), 882-884.

2. (a) Weighardt, K.; Pohl, K.; Jibril, I.; Huttner, G. *Angew. Chem. Int. Ed.* **1984,** *23* (1), 77-78; (b) Barra, A. L.; Debrunner, P.; Gatteschi, D.; Schulz, C. E.; Sessoli, R. *Europhys. Lett.* **1996,** *35* (2), 133-138; (c) Aromi, G.; Brechin, E. K. *Struct. Bonding (Berlin, Ger.)* **2006,** *122*, 1-67; (d) Rodriguez, E.; Gich, M.; Roig, A.; Molins, E.; Nedelko, N.; Slawska-Waniewska, A.; Szewczyk, A. *Polyhedron* **2006,** *25* (1), 113-118.

3. (a) Boudalis, A. K.; Sanakis, Y.; Raptopoulou, C. P.; Terzis, A.; Tuchagues, J.-P.; Perlepes, S. P. *Polyhedron* **2005,** *24* (12), 1540-1548; (b) Raptopoulou, C. P.; Sanakis, Y.; Boudalis, A. K.; Psycharis, V. *Polyhedron* **2005,** *24* (5), 711-721.

4. (a) Murray, K. S. *Coord. Chem. Rev.* **1974,** *12* (1), 1-35; (b) Shiemke, A. K.; Loehr, T. M.; Sanders-Loehr, J. *J. Am. Chem. Soc.* **1986,** *108* (9), 2437-43; (c) Que, L., Jr.; True, A. E. *Prog. Inorg. Chem.* **1990,** *38*, 97-200; (d) Kurtz, D. M. Jr. *Chem. Rev.* **1990,** *90* (4), 585-606; (e) Wilkins, R. G., Binuclear iron centers in proteins. *Chem. Soc. Rev.* **1992,** *21* (3), 171-8; (f) Solomon, E. I.; Zhang, Y. *Acc. Chem. Res.* **1992,** *25* (8), 343-52.

5. Mason, K.; Chang, J.; Prescimone, A.; Garlatti, E.; Carretta, S.; Tasker, P. A.; Brechin, E. K. *Dalton Trans.* **2012,** *41* (29), 8777-8785.

6. Thorpe, J. M.; Beddoes, R. L.; Collison, D.; Garner, C. D.; Helliwell, M.; Holmes, J. M.; Tasker, P. A. *Angew. Chem. Int. Ed.* **1999,** *38* (8), 1119-1121.

7. (a) Gass, I. A.; Milios, C. J.; Collins, A.; White, F. J.; Budd, L.; Parsons, S.; Murrie, M.; Perlepes, S. P.; Brechin, E. K. *Dalton Trans.* **2008,** (15), 2043-2053; (b) Mason, K.; Gass, I. A.; Parsons, S.; Collins, A.; White, F. J.; Slawin, A. M. Z.; Brechin, E. K.; Tasker, P. A. *Dalton Trans.* **2010,** *39* (10), 2727-2734; (c) Mason, K.; Chang, J.; Garlatti, E.; Prescimone, A.; Yoshii, S.; Nojiri, H.; Schnack, J.; Tasker, P. A.; Carretta, S.; Brechin, E. K. *Chem. Commun.* **2011,** *47* (21), 6018-6020; (d) Holynska, M.; Clerac, R.; Langer, T.; Poettgen, R.; Dehnen, S. *Polyhedron* **2013,** *52*, 1425-1430; (e) De Silva, D. N. T.; Dais, T. N.; Jameson, G. B.; Cutler, D. J.; Brechin, E. K.; Davies, C. G.; Jameson, G. N. L.; Plieger, P. G. *ACS Omega* **2021,** *6* (25), 16661-16669.

8. Wenzel, M.; Forgan, R. S.; Faure, A.; Mason, K.; Tasker, P. A.; Piligkos, S.; Brechin, E. K.; Plieger, P. G. *Eur. J. Inorg. Chem.* **2009,** *2009* (31), 4613-4617.

9. (a) Aldred, R.; Johnston, R.; Levin, D.; Neilan, J. *J. Chem. Soc. Perkin Trans. 1* **1994,** (13), 1823-31; (b) Stevens, J. R.; Plieger, P. G. *Dalton Trans.* **2011,** *40* (45), 12235-12241; (c) Forgan, R. S.; Davidson, J. E.; Galbraith, S. G.; Henderson, D. K.; Parsons, S.; Tasker, P. A.; White, F. J. *Chem. Commun.* **2008,** (34), 4049-4051.

10. Murad, E.; Cashion, J. (Eds.) *Mössbauer Spectroscopy of Environmental Materials and Their Industrial Utilization*. Kluwer Academic, 2004; p440.

Article

Review of non-macrocyclic triangular M_3Ln complexes

BRODIE E. MATHESON* AND TYSON N. DAIS

School of Natural Sciences, Massey University, Palmerston North
(Email: b.matheson@massey.ac.nz)

Keywords: *tetranuclear-clusters, triangle complexes, 3d-4f SMMs*

Introduction

Since the discovery of slow relaxation of magnetisation in the archetypal Mn_{12} single molecule magnet (SMM) in 1993 by Sessoli et al.,[1] the study and application of molecular magnetism has grown remarkably. SMMs are discrete molecules that are capable of being magnetised and retaining this magnetisation below a certain temperature known as the blocking temperature k_BT. Unlike traditional bulk magnets, the origin of the magnetic properties within SMMs is purely molecular in nature, rather than due to long-range ordering effects. There are two common types of SMMs described in the literature; mononuclear complexes, also known as single-ion magnets (SIMs)[2-4] and polynuclear complexes, which can be either homo-[5-7] or heterometallic.[8-10]

A decade after the report of Mn_{12}, the first lanthanide based SMM was reported, $[LnPc_2]$.[11] The lanthanide metals have large ground state magnetic anisotropies and spin multiplicities, which helps prevent reversal of magnetisation.[12] However, lanthanide ions suffer from quantum tunnelling of the magnetisation, which bypasses the energy barrier preventing the reversal of magnetisation. The inclusion of 3d metals linked by a bridging ligand to 4f ions establishes magnetic exchange pathways which can act to suppress the quantum tunnelling of magnetisation leading to more desirable magnetic behaviour.[13,14]

Design

A majority of reported SMMs focussed on the unpredictable outcome of reacting small multidentate ligands or larger and more flexible chelating ligands with arbitrary ratios of each metal.[15-17]

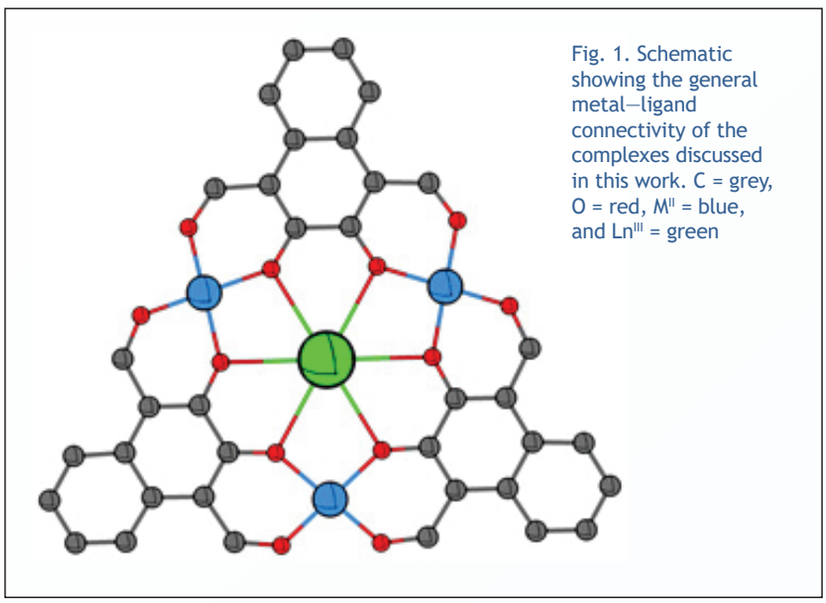

Fig. 1. Schematic showing the general metal–ligand connectivity of the complexes discussed in this work. C = grey, O = red, M^{II} = blue, and Ln^{III} = green

Symmetric di-substituted catechol-based ligands were first utilised by Nabeshima et al. to generate a Zn_3La complex in the form of a macrocyclic molecular triangle with a planar M_3LnO_6 core, for the purposes of increasing the yield of their previously reported metal-free 3 + 3 macrocyclisation.[18] The use of 1,4- diformylbenzene-2,3-diol in combination with various diamines was later shown by Brooker et al.[19-22] to reliably generate analogous complexes of the triangular M_3Ln topology with potentially interesting magnetic properties. A similar family of non-macrocyclic M_3Ln 'star' shaped clusters, which contain non-planar M_3LnO_6 cores, has also been well established within the literature.[23-25]

In this review we discuss a few examples from the recently reported additions to the non-macrocyclic triangle topology, using the larger acyclic ligand 1,4-diformylnaphthalene-2,3-diol (H_2L), to include non-macrocyclic Cu_3Ln,[26] Ni_3Ln,[27] and Co_3Ln[28] triangles as well as explore their magnetic properties.

Synthesis

All L_3M_3Ln complexes discussed here were prepared from a 3:3:1 mixture of methanolic solution of the nitrate salt of the corresponding transition metal, a lanthanide salt, and the ligand, (H_2L). Addition of the transition metal solution in all cases caused rapid dissolution of the ligand suspension regardless of order of addition, the same effect was not observed when the lanthanide solution was added prior to the transition metal solution. IR spectroscopy of the resulting complexes revealed a new band in the 1610 – 1616 cm^{-1} region corresponding to the coordinated aldehyde groups, with no

bands corresponding to unreacted aldehyde (1673 and 1641 cm^{-1}) present after complexation.

X-ray characterisation

Single crystal X-ray diffraction studies revealed the expected (based on literature examples of analogous macrocycles), L_3M_3Ln structural motif (Fig. 1). This structure was present for all complexes discussed here.

Each lanthanide is bound equatorially in an O_6 environment by three catecholate (equivalent to six phenolate) groups in an approximately planar arrangement. The prearrangement of the three ligand molecules around the lanthanide centre brings the aldehyde groups into proximity like the imine nitrogens of a salen moiety (Fig. 1). The two adjacent aldehyde and phenolate groups form an O_4 environment to bind to the equatorial sites of the transition metal centres while the remaining axial coordination sites of each metal are bound by a mixture of solvent molecules or anions.

The copper-terbium complex C1 (Fig. 2) crystallised in monoclinic space group $P2_1$, and single crystal X-ray diffraction revealed a relatively non-planar arrangement of ligands with a mixture of nitrate and chloride caps on the metal centres. The Tb^{III} centre sits in the middle of the O_6 equatorial binding environment with its axial sites occupied a η_2-NO_3 anion on one side of the Cu3 plane, and by two water molecules on the other side of the plane, making it ten coordinate.

Each Cu^{II} centre adopts a square pyramidal geometry with the equatorial sites occupied by a phenol and an aldehyde each from two ligand units. The copper centres are axially capped by either a chloride (Cu1 and Cu2) or a methanol molecule (Cu3), with all three copper ions being capped on the same side of the Cu_3 plane. The entire bridging ligand between Cu1 and Cu3 sits below the Cu_3 plane, while the remaining two bridging ligands form a separate plane, and the terbium centre is displaced above the Cu3 plane by 0.162(3) Å.

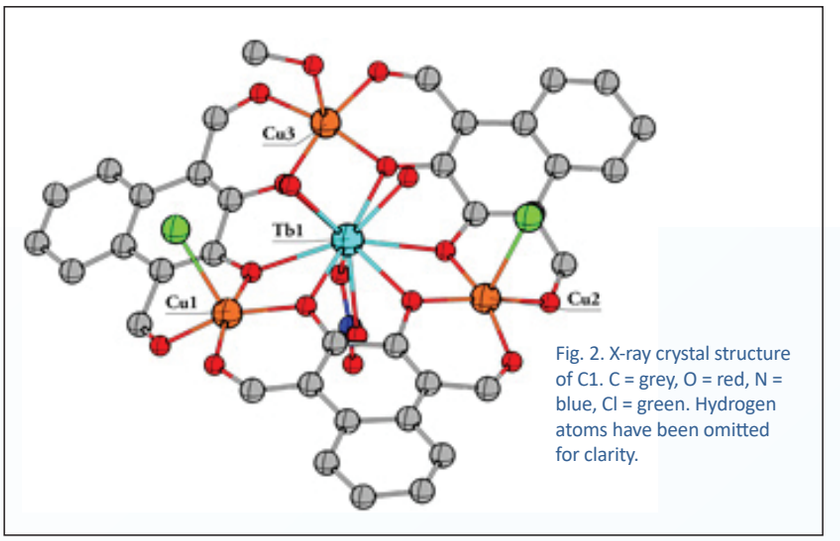

Fig. 2. X-ray crystal structure of C1. C = grey, O = red, N = blue, Cl = green. Hydrogen atoms have been omitted for clarity.

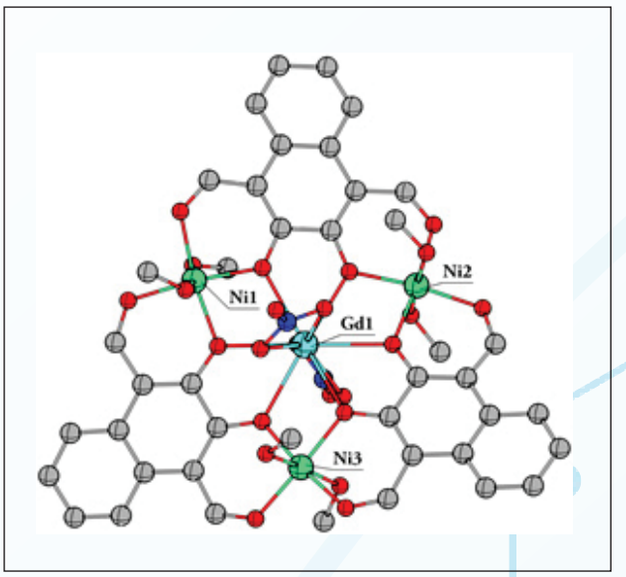

Fig. 3. X-ray crystal structure of C2. C = grey, O = red, N = blue. Hydrogen atoms have been omitted for clarity.

The nickel-gadolinium complex, C2 (Fig. 3), crystallised in the primitive monoclinic space group $P2_1/n$. Each Ni^{II} centre adopts a regular octahedral geometry with the equatorial sites occupied by the phenolate and aldehyde groups of L and methanol groups coordinating axially.

The La^{III} centre is ten coordinate with six equatorial sites occupied by the phenolate groups of L as well as two axially coordinated η_2-NO_3 molecules. C2 contains a trivalent lanthanide centre, thus required an additional monoanionic counterion to be present, which was crystallographically identified as a non-coordinated nitrate anion (not shown in Fig. 3).

The cobalt-lanthanum complex C3 (Fig. 4) crystallised in the $P\bar{1}$ space group. It contains two cobalt centres with near perfect octahedral geometry (Co1 and Co2). Both Co1 and Co2 have the equatorial sites occupied by the phenolate and aldehyde groups of L and are axially coordinated by water molecules.

In contrast, Co3 has only a single axially coordinated water molecule resulting in a five-coordinate distorted D_{3h} trigonal bipyramidal coordination geometry. The La^{III} centre is 11

coordinate with six equatorial sites occupied by the phenolate groups of L as well as two η_2-NO_3 groups and a water molecule, resulting in an approximate C_{5v} symmetry of a capped pentagonal antiprism. The final negative charge required to balance the +9 charge of the metal centres, as in C2, is present as a non-coordinated nitrate anion (not shown in Fig. 4).

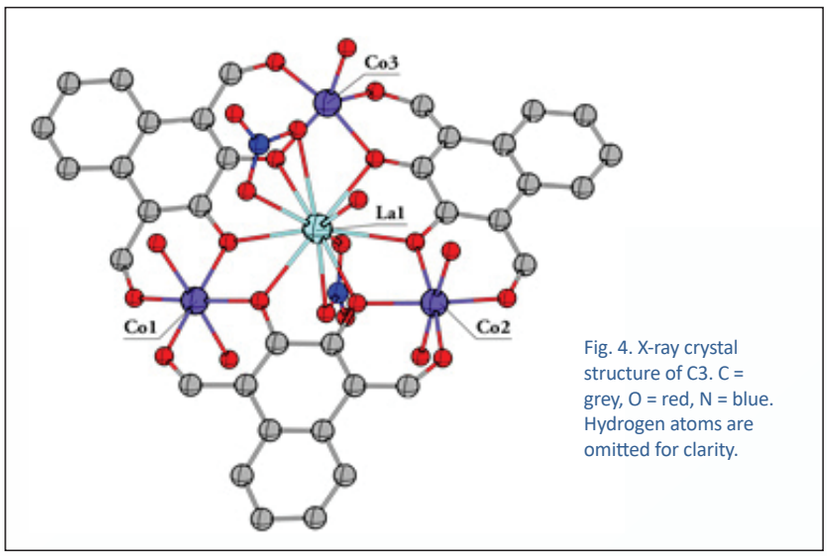

Fig. 4. X-ray crystal structure of C3. C = grey, O = red, N = blue. Hydrogen atoms are omitted for clarity.

Magnetic properties

Magnetic characterisation of each of the reported complexes was also undertaken. Macrocyclic analogues indicated that the Tb^{III} centred complex, C1, was likely to exhibit SMM properties. Experimentally, C1 exhibited a sharp increase in the DC magnetic susceptibility when cooled below 50 K, reaching a peak of 14.6 cm^3 K mol^{-1} at 2.2 K This peak strongly suggests ferromagnetic coupling between the Tb^{III} and Cu^{II} centres and indicated a high spin ground state of $S_{total}=S_{TbIII}+3S_{CuII}=6/2+3/2+9/2$ AC magnetic susceptibility measurements indicated C1 exhibited slow relaxation of magnetisation below ca. 5 K (Fig. 5), which is crucial for an SMM. Complex C1 has an odd number of unpaired electrons, so is classified as a Kramers type molecule and had an observable barrier to relaxation even with zero applied bias. The maximum barrier to the reversal of magnetisation was determined to be 13.3(2) K in a weak applied field.

DC magnetic susceptibility measurements indicated the three Ni^{II} centres in C2 were ferromagnetically coupled to the central Gd^{III} ion with a calculated coupling constant of $2J/k_B$ = 1.6 – 2.0 K. The zero-field splitting effect was found to lead to a decrease of the magnetic susceptibility, which was particularly evident in the low-temperature region.

The AC magnetic susceptibility of C2 was also investigated; however, no appreciable frequency dependent signals were observed. It is interesting to note that Gd^{III} complexes generally do not behave as SMMs because of its magnetically isotropic nature, but related analogues containing heavier lanthanide ions could be prepared by means of the same synthetic strategy.

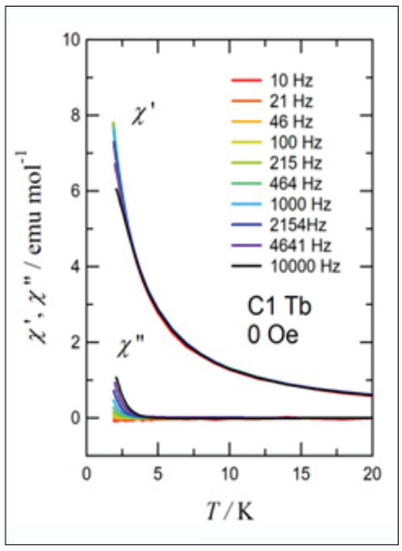

Fig. 5. Temperature and frequency dependence of the real (*x'*) and imaginary (*x''*) AC magnetic susceptibilities in zero applied DC field.

Since La^{III} has a $[Xe]4f^0$ electron configuration, it is diamagnetic, so DC magnetic susceptibility and magnetisation measurements of C3 were completed to examine the potential Co—Co interactions and/or zero-field splitting effects.

Fig. 6A shows the DC magnetic susceptibility reaching 9.4 cm^3 K mol^{-1} at 300 K, which indicated the three Co^{II} centres were high spin, i.e. $S_{CoII}=3/2$ with a g-value of 2.59. The experimental magnetisation (Fig. 6B) at 7 T was 7.1 μ_B, which corresponds to only about 60% of the theoretical upper limit (11.7 μ_B).

"Gd^{III} complexes generally do not behave as SMMs because of its magnetically isotropic nature, but related analogues containing heavier lanthanide ions could be prepared by means of the same synthetic strategy."

If antiferromagnetic interactions were dominant, the experimentally measured magnetisation would be approximately one third of the theoretical value and the DC magnetic susceptibility at 1.8 K would approach one third of the value at 300 K. Hence the measured value of 7.1 μ_B indicates antiferromagnetic interactions are relatively small for this system. This means two cobalt centres have spins which are parallel to each other, while the third is antiparallel.

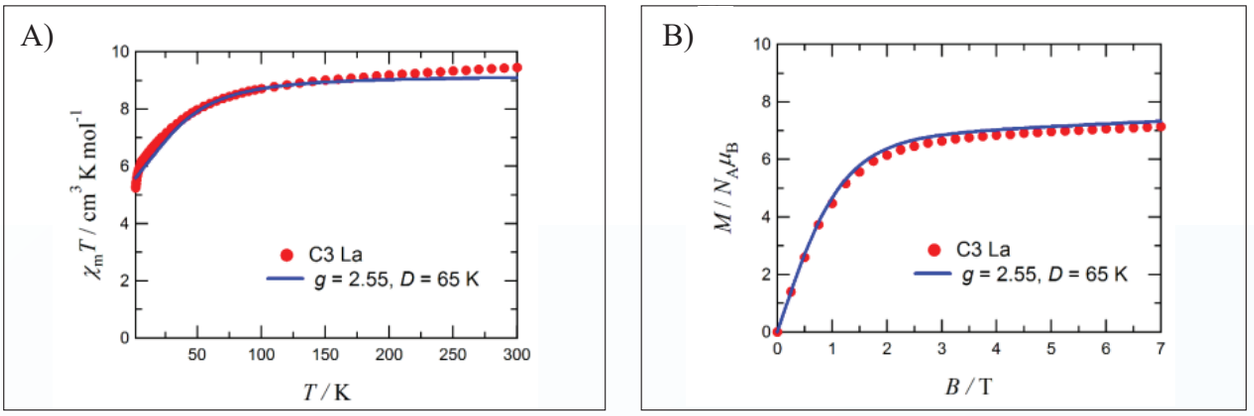

Fig. 6. Plot of DC magnetic susceptibility (xmT vs T) for C3 measured at 0.5 T (A) and the DC magnetisation (M vs H) plot for C3 measured at 1.8 K, including calculated fits and parameters.

Conclusions

While these recently published non-macrocyclic triangle complexes provide new examples of this topology in the literature, and magnetic characterisation of the resulting complexes shows the potential of this topology for use in the synthesis of SMMs, there are still many more interesting metal combinations to be explored. The successful self-assembly of iron or manganese containing triangles with heavy lanthanide ions would make an interesting pathway for exploration.

References

1. Sessoli, R.; Gatteschi, D.; Caneschi, A.; Novak, M. *Nature* **1993**, *365* (6442), 141–143.
2. Blackaby, W. J. M.; Sabater, S.; Poulten, R. C.; Page, M. J.; Folli, A.; Krewald, V.; Mahon, M. F.; Murphy, D. M.; Richards, E.; Whittlesey, M. K. *Dalton Trans*. **2018**, *47*, 769–782.
3. Hay, M. A.; Sarkar, A.; Craig, G. A.; Marriott, K. E. R.; Wilson, C.; Rajaraman, G.; Murrie, M. *Chem. Commun*. **2020**, *56*, 6826–6829.
4. Liu, J.; Chen, Y.-C.; Liu, J.-L.; Vieru, V.; Ungur, L.; Jia, J.-H.; Chibotaru, L. F.; Lan, Y.; Wernsdorfer, W.; Gao, S.; Chen, X.-M.; Tong, M.-L. *J. Am. Chem. Soc.* **2016,** *138*, 5441–5450.
5. Papatriantafyllopoulou, C.; Moushi, E. E.; Christou, G.; Tasiopoulos, A. J. *Chem. Soc. Rev*. **2016**, *45,* 1597–1628.
6. Escuer, A.; Esteban, J.; Perlepes S. P.; Stamatatos, T. C. *Coord. Chem. Rev*. **2014**, *275,* 87–129.
7. Woodhouse, S. S.; Dais, T. N.; Payne, E. H.; Singh, M. K.; Brechin, E. K.; Plieger, P. G. *Dalton Trans*. **2021**, *50,* 5318–5326.
8. Chakraborty, A.; Goura, J.; Bag P.; Chandrasekhar, V. *Eur. J. Inorg. Chem*. **2019**, *2019,* 1180–1200.
9. Xue, S.; Guo, Y.-N.; Zhao, L.; Zhang, H.; Tang, J. *Inorg. Chem*. **2014**, *53,* 8165–8171.
10. Langley, S. K.; Wielechowski, D. P.; Vieru, V.; Chilton, N. F.; Moubaraki, B.; Chibotaru, L. F.; Murray, K. S. *Chem. Commun*. **2015**, *51,* 2044–2047.
11. Ishikawa, N.; Sugita, M.; Ishikawa, T.; Koshihara, S.; Kaizu, Y. *J. Am. Chem. Soc.* **2003**, *125* (29), 8694–8695
12. Chen, Y.-C.; Huang, X.-S.; Liu, J.-L.; Tong, M.-L. *Inorg. Chem.* **2018**, *57* (18), 11782–11787.
13. Wang, H.-L.; Zhu, Z.-H.; Peng, J.-M.; Zou, H.-H. *J. Clust. Sci.* **2021**.
14. Liu, K.; Shi, W.; Cheng, P. *Coord. Chem. Rev.* **2015**, *289*, 74–122
15. Jurca, T.; Farghal, A.; Lin, P.-H.; Korobkov, I.; Murugesu, M.; Richeson, D. S. *J. Am. Chem. Soc*. **2011**, *133,* 15814– 15817.
16. Peng, M.; Wu, X.-F.; Wang, L.-X.; Chen, S.-H.; Xiang, J.; Jin, X.-X.; Yiu, S.-M.; Wang, B.-W.; Gao, S.; Lau, T.-C. *Dalton Trans*. **2021**, *50,* 15327–15335.
17. Tasiopoulos, A. J.; Vinslava, A.; Wernsdorfer, W.; Abboud, K. A.; Christou, G. *Angew. Chem*. **2004**, *116,* 2169–2173.
18. Akine, S.; Sunaga, S.; Taniguchi, T.; Miyazaki, H.; Nabeshima, T. *Inorg. Chem*. **2007**, *46,* 2959–2961.
19. Feltham, H. L. C.; Clerac, R.; Powell, A. K.; Brooker, S. *Inorg. Chem*. **2011**, *50,* 4232–4234.
20. Feltham, H. L. C.; Clerac, R.; Ungur, L.; Chibotaru, L. F.; Powell, A. K.; Brooker, S. *Inorg. Chem*. **2013**, *52,* 3236– 3240.
21. Feltham, H. L. C.; Clerac, R.; Ungur, L.; Vieru, V.; Chibotaru, L. F.; Powell, A. K.; Brooker, S. *Inorg. Chem*. **2012**, *51,* 10603–10612.
22. Feltham, H. L. C.; Dhers, S.; Rouzieres, M.; Clerac, R.; Powell, A. K.; Brooker, S. *Inorg. Chem. Front*. **2015**, *2,* 982–990.
23. Chilton, N. F.; Langley, S. K.; Moubaraki, B.; Murray, K. S. *Chem. Commun*. **2010**, *46,* 7787–7789
24. Kettles, F. J.; Milway, V. A.; Tuna, F.; Valiente, R.; Thomas, L. H.; Wernsdorfer, W.; Ochsenbein, S. T.; Murrie, M. *Inorg. Chem*. **2014**, *53,* 8970–8978.
25. Efthymiou, C. G.; Stamatatos, T. C.; Papatriantafyllopoulou, C.; Tasiopoulos, A. J.; Wernsdorfer, W.; Perlepes S. P.; Christou, G. *Inorg. Chem*. **2010**, *49,* 9737–9739.
26. Dais, T. N.; Takano, R.; Yamaguchi, Y.; Ishida, T.; Plieger, P. G. *ACS Omega* **2022**, *accepted manuscript*, DOI: 10.1021/acsomega.1c07001.
27. Dais, T. N.; Takano, R.; Ishida, T.; Plieger, P. G. *Dalton Trans*. **2022**, *51,* 1446–1453.
28. Dais, T. N.; Takano, R.; Ishida, T.; Plieger, P. G. *RSC Adv.* **2022**, *accepted manuscript*.

Article

Small metal cation coordination of quinolino [7,8-*h*]quinoline derivatives

PAUL G. PLIEGER

School of Natural Sciences, Massey University, Palmerston North
(Email: p.g.plieger@massey.ac.nz)

Keywords: *boron, beryllium, quinolino [7,8-h] quinoline, complex*

Introduction

Since I first caught sight of quinolino[7,8-*h*]quinoline (QQ, Fig. 1) as a post-doctoral fellow, I have been fascinated by this little molecule and its possibilities. At the time I was searching for potential chelators for beryllium(II) and I thought this molecule had potential to bind beryllium with some selectivity. My interest in beryllium stems from the fact that due to its inherent high toxicity (it is a class I carcinogen) and high health risk (dust particles of beryllium salts can lead to chronic beryllium disease, a sometimes-fatal lung disease[1,2]), it is very understudied as an element. Currently, no ligand exists that is a strong and selective chelator for beryllium.

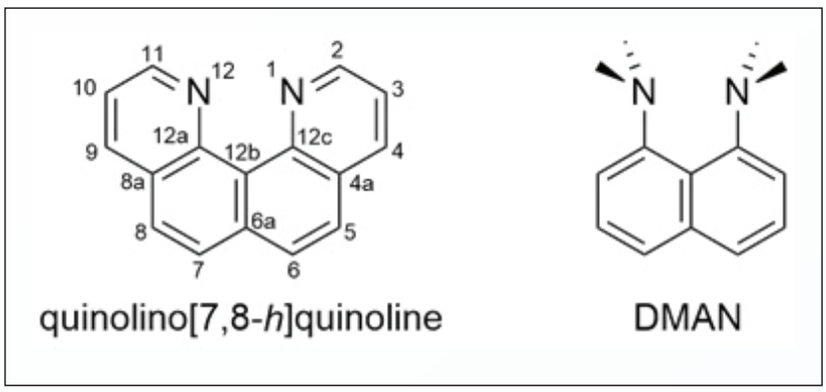

Fig. 1. Quinolino[7,8-h]quinoline (QQ) showing the atom numbering scheme and 1,8-bis(dimethyl aminonaphthalene) (DMAN)

Quinolino[7,8-*h*]quinoline (**QQ**) is closely related to 1,8-bis(dimethylamino) naphthalene (DMAN), (Fig. 1), the original Proton Sponge®.[3] Both molecules possess lone pairs of electrons on the proximal nitrogen atoms which cause a destabilising electrostatic interaction that can be alleviated by the coordination of a proton. The neutral species of 4,9-dichloroquinolino[7,8-*h*]quinoline (**QQ-Cl$_2$**) displays helical distortions to remove this lone pair interaction, while the protonated species becomes planar (Fig. 2).

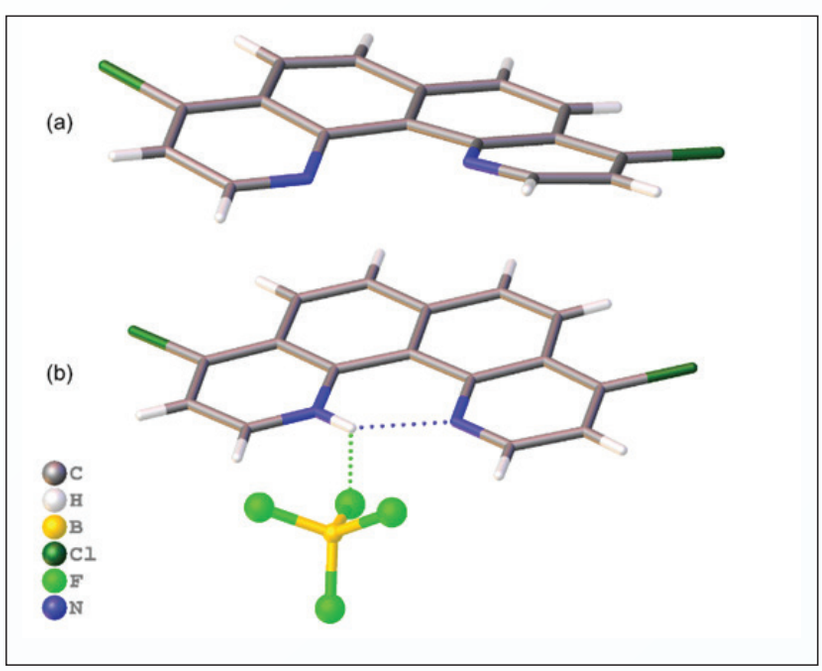

Fig. 2. X-ray structure pictures of (a) neutral and (b) protonated forms of 4,9-dichloroquinolino[7,8-h]quinoline (QQ-Cl$_2$). Refer to Fig. 1 for the key to the atom numbering scheme. Chloroform solvent molecules for (a) have been removed for clarity.

For both DMAN and QQ, few coordination chemistry studies have been reported.[4-9] For instance, only one complex of non-substituted DMAN has been published.[10] This is possibly due to the difficulty of forming stable complexes with this ligand as the methyl groups cause unfavourable interactions which destabilise the resulting metal complexes. However, this is not an issue for the quinolino-quinoline system. By including the nitrogen donors in an aromatic system, the destabilising steric effects of the methyl groups have been removed. Despite this advantage, very few complexes have been reported for quinolino[7,8-*h*]quinoline or any of its derivatives in the last three decades.[5-8] This is likely due to a couple of factors. The first is the difficulty in synthesising the molecule or any of its derivatives in any reasonable

amount. At present the synthesis is a multi-step linear progression, with most derivatives generated from the dihalide quinolinoquinoline. While some advances in its synthesis have been achieved,[11-12] obtaining large quantities of the molecule is also still problematic. The second relates to coordination environment. While both nitrogen atoms are available for coordination, forming a nice stable six-membered chelate ring, their close proximity means there is little room available to accommodate anything but the smallest metallic cations.

In the few examples of quinolinoquinoline complexes that contain medium to larger sized cations, there is considerable curvature of the ligand and large out-of-plane metal-ligand displacements present to accommodate the chelation to both nitrogen donor atoms. There is a suggestion that these complexes could make useful catalyst precursors.[5,7] Given my interest in both beryllium and this molecule my research group set about to explore the coordination aspects of this ligand with smaller metallic cations.

Complexes of boron

Our initial studies began with both boron and beryllium. Both are small ionic radii metallic elements with typical oxidation states of +3 for boron and +2 for beryllium. The success of the beryllium complex studies (which were done at Los Alamos National Laboratory) were rather inconclusive, largely because we were restricted to aqueous beryllium starting materials.

Trying to coordinate a proton sponge-like material to a weakly coordinating cation in the presence of a large concentration of a polar protic solvent was always going to be 'challenging'. This proved to be the case with all spectral data obtained for the complexation attempts indistinguishable from that of the protonated forms of the quinolinoquinoline ligand. We overcame this limitation by switching to aprotic solvents some years later with a new collaborator in Germany (see next section).

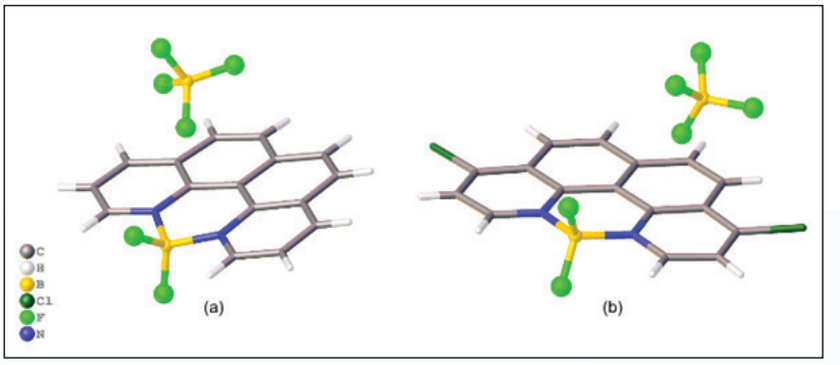

Fig. 3. X-ray structure pictures of the BF_2 containing tetrafluoroborate complexes for (a) QQ and (b) QQ-Cl_2

"Trying to coordinate a proton sponge-like material to a weakly coordinating cation in the presence of a large concentration of a polar protic solvent was always going to be 'challenging'."

The boron chemistry we could do locally, and complexes were obtained by the reaction of boron trifluoride etherate in acetonitrile to form two BF_2 adducts of the 4,9-dichloro- (**QQ-Cl_2**) and unsubstituted quinolinoquinoline (**QQ**) as tetrafluoroborate salts.[6] The reaction with 4,9-dichloroquinolinoquinoline did not proceed cleanly, but the (subsequently identified) protonated form of the ligand was easily able to be separated. Full characterisation followed including single crystal structural analysis (Fig. 3).

Description of the crystal structures of the boron complexes

Each complex exhibited similar features, namely the boron atom sat in a tetrahedral coordination environment sandwiched between two nitrogen donor atoms of the ligand, with fluoride atoms completing the coordination sphere. We were delighted to see that the fit of the boron to the chelation site was excellent in both cases, with the boron ion located only slightly above the mean plane (N1, C12c, C12b, C12a, N12) of the fully conjugated ligand (0.186(4) Å for $[BF_2QQ]^+$, Fig. 3a and 0.096(6) Å for $[BF_2QQ\text{-}Cl_2]^+$, Fig. 3b), thus the binding pocket of these ligands appeared to be an ideal size to support the small B^{III} cation.

Spectroscopic studies of the boron complexes

The UV-Vis spectra for the neutral, protonated and coordinated complexes all exhibited similar and somewhat unremarkable features. Specifically, $\pi - \pi^*$ transitions dominate at <400 nm in all spectra recorded. Likewise, fluorescence studies were also somewhat fruitless with only weak fluorescence intensities observed for the chlorinated complex (and dichloro-protonated ligand), indicating that weak charge transfer between the chloride atoms and the aromatic heterocycle was the most likely source of the fluorescence.

Complexation with beryllium

In more recent years, our group has enjoyed a productive collaboration with Dr Magnus Buchner at the University of Marburg, who has developed beryllium halide staring materials that can be used in non-aqueous solvent environments. While this now gave us a fighting chance to coordinate to the quinolinoquinoline compounds, very poor solubility of the resulting products was problematic. We attempted beryllium coordination with several quinolinoquinoline derivatives.[8] The 4,9-dibromo- (QQ-Br_2) and 4,9-dichloro- (QQ-Cl_2) derivatives (as used to coordinate boron) were subjected to complexation attempts with beryllium but both resulted in insoluble solids (using dichloromethane) with no discernible signals in any NMR spectra, or, simple beryllium halide acetonitrile adducts (using acetonitrile) as indicated from ^{1}H, ^{13}C and ^{9}Be NMR spectra. However, complexation reactions with the derivative 4,9-dihydroxyquinolino[7,8-h]quinoline (QQ-$(OH)_2$) revealed a new ^{9}Be NMR signal which was subsequently assigned as the complex. This particular ligand derivative exists in a keto-enol form which is slightly more energetically favoured but undergoes tautomerism to the enol-enol form upon coordination (Fig. 4).

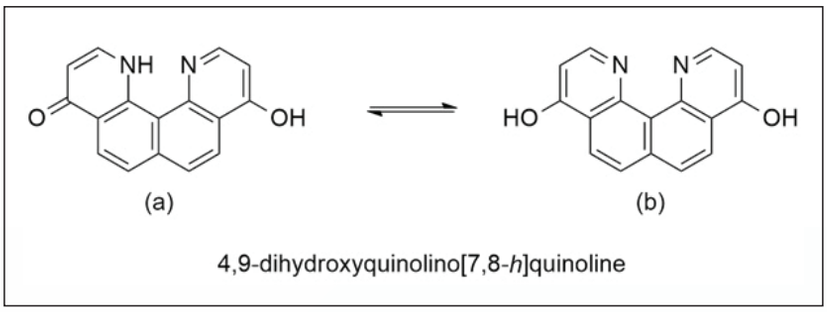

Fig. 4. The 4,9-dihydroxyquinolino[7,8-h]quinoline derivative (QQ-$(OH)_2$) shown as the (a) keto-enol and (b) enol-enol forms

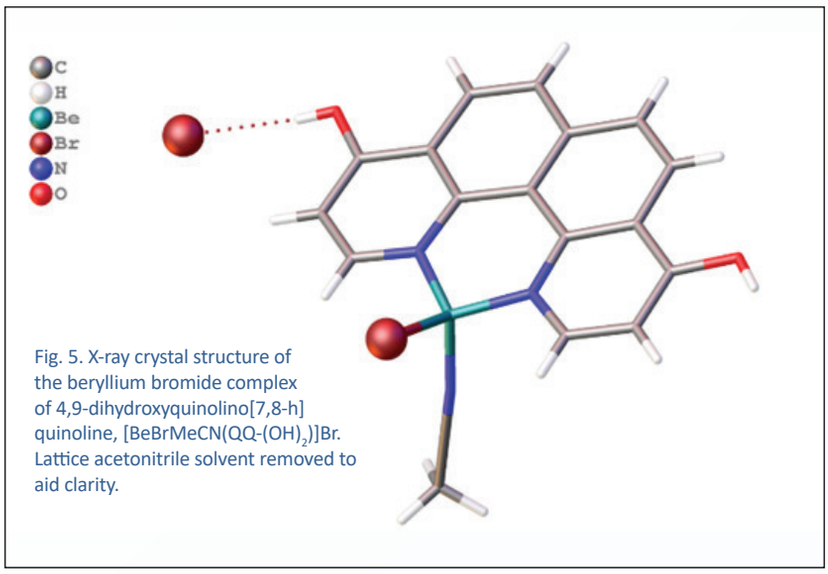

Fig. 5. X-ray crystal structure of the beryllium bromide complex of 4,9-dihydroxyquinolino[7,8-h] quinoline, [BeBrMeCN(QQ-$(OH)_2$)]Br. Lattice acetonitrile solvent removed to aid clarity.

The solution chemistry of this system with the beryllium halide starting material is quite dynamic, resulting in very complex ^{1}H and ^{13}C spectra. We were therefore very fortunate to develop a method for obtaining single crystals of the beryllium complex. By heating a suspension of the complex in acetonitrile at 90 °C for two weeks we obtained single crystals suitable for X-ray analysis, thus providing structural proof of the successful coordination (Figure 5).

Description of the crystal structure of the beryllium complex

The complex features a beryllium atom in a tetrahedral coordination environment, with an acetonitrile ligand, a bromide ligand and two N atoms of the quinolinoquinoline derivative making up the coordination sphere (Fig. 5). The ligand is in the di-enol tautomeric form of 4,9-dihydroxyquinolino[7,8-*h*]quinoline. The crystal structure of the complex features an acetonitrile solvent molecule and a bromide counter ion from the beryllium halide salt, with the bromide counter ion forming hydrogen bonds with hydroxy groups of adjacent molecules of the complex.

Spectroscopic studies of the beryllium complex

Due to the inherent toxicity of beryllium we were fairly restricted in what we could achieve. Several further NMR and ATR-FTIR spectroscopic measurements were undertaken, as were some preliminary fluorescence experiments on all of the products from the complex reactions. Again, we were plagued by low solubility, resulting in less than satisfactory results. To further evaluate the species in solution, reactions QQ-$(OH)_2$, QQ-Cl_2 and QQ-Br_2 with $BeCl_2$ and $BeBr_2$ salts were conducted in pyridine-d_5.

Again, mostly insoluble solids were obtained, or detection of solvent adducts of the starting salts with no signs of coordination to the ligands for the halogen substituted variants. For the QQ-$(OH)_2$, the results were slightly more encouraging with a new ^{9}Be signal tentatively assigned to the neutral complex [$BeCl_2$(QQ-$(OH)_2$)].

Further experiments with the strongly coordinating solvent dimethylformamide (dmf) and BeI_2 also gave rise to a new signal which was tentatively assigned to the cation [Be(dmf)$_2$(QQ-

$(OH)_2)]^{2+}$. As quinoquinoline complexes are known to show fluorescence,[11] some quick preliminary tests under UV light were undertaken. They revealed significantly different colours for the chloro- and bromo- beryllim salts with QQ-$(OH)_2$ (Fig. 6).

So which metallic cation appears to have the best fit within this ligand? We have attempted to quantify this by looking at various structural parameters of the ligand (Table 1). It is complicated slightly by the lack of comparable data from a single derivative, but the general trend does suggest that the **QQ** ligands are a very good fit for both boron and beryllium.

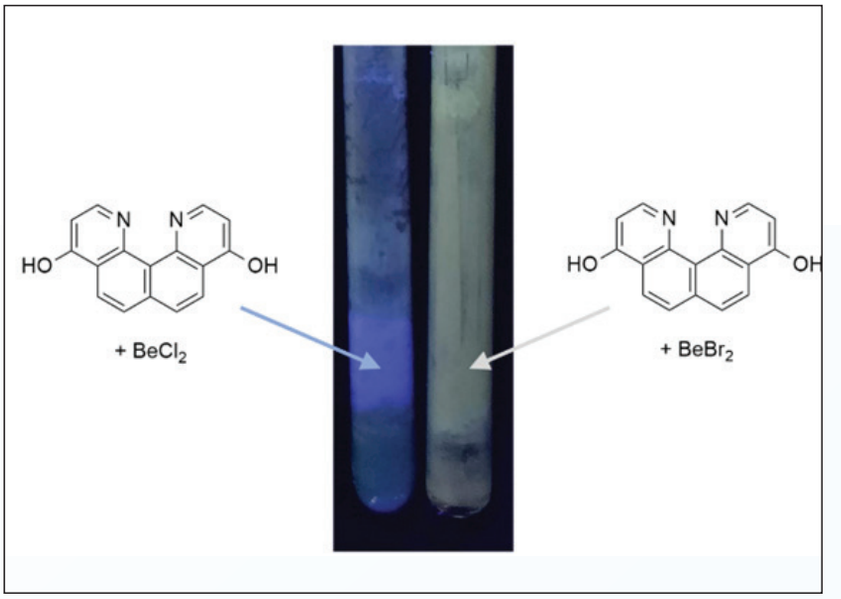

Fig. 6. Precipitates from the reactions of $BeCl_2$ and $BeBr_2$ with QQ-$(OH)_2$ in pyridine-d_5 under UV light

As mentioned before, the non-protonated neutral compound **QQ-Cl_2**, has the widest N···N distance and greatest torsional angle as the molecule attempts to relieve the nitrogen electron lone pair-lone pair interactions. Protonation of the ligand provides that relief as evidenced by the reduction in the N1-N12 and C12a-C12c distances and no deviation in terms of torsional twist or out-of-plane (OOP) displacement of the H-bonded proton. Essentially the molecule has become extremely flat. Replacing the proton with the more highly charged B^{3+} ion has resulted in a further contraction in the N1-N12 and C12a-C12c distances, but little change in the distance of the outer carbons of the ring (C6-C7).

The torsional angle and OOP have both increased, however, indicating a poorer size match. Changing to the larger Be^{2+} cation (albeit with the **QQ-$(OH)_2$** derivative now), has increased the N1-N12 and C12a-C12c distances to an approximately intermediate value between that of the neutral complex and the protonated forms of the **QQ-Cl_2** compound.

Surprisingly, however, the OOP distance of the cation from the mol-

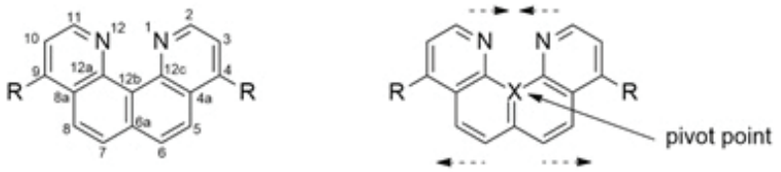

4,9-disubstituted quinolino[7,8-*h*]quinoline

Compound	Atomic distances (Å)				Torsion angle (°)	Ref.
	N1-N12	C12a-C12c	C6-C7	OOP *X*-plane [a]	N1-C12c-C12a-N12	
QQ-Cl_2	2.768(2)	2.585(2)	2.444(2)	–	20.02	6
[QQ-Cl_2H]$^+$	2.591(2)	2.539(3)	2.467(3)	0.001	0.17	6
[BF_2(QQ)]$^+$	2.560(3)	2.500(4)	2.470(4)	0.186	2.43	6
[BF_2(QQ-Cl_2)]$^+$	2.551(5)	2.511(5)	2.467(7)	0.098	1.16	6
[BeBrMeCN(QQ-$(OH)_2$)]$^+$	2.703(2)	2.561(2)	2.449(2)	0.092	0.92	8

Table 1. Selected atomic distances and torsion angles for compounds of QQ and derivatives [a] Out of plane cation displacement relative to the ligand. X is H^+, $B3^+$ or $Be2^+$ and the plane consists of N1, C12c, C12b, C12a and N12 atoms.

ecule and torsional angle is less than either of the boron complexes, suggesting that the beryllium does a better job at relieving the lone pair-lone pair stress of the molecule.

Overall, the quinolino[7,8-h]quinoline motif seems to possess a 'just-right' chelate size for Be(II) coordination. This is shown by the formation of highly stable, though very insoluble, beryllium compounds, in which the quinolino[7,8-*h*]quinolone ligands can only be displaced by strong donor solvents if a massive excess of these is present.

Concluding remarks

This fundamental project has been a 'back-burner' project since I started my academic career and has been a lot of fun. I still find the quinolino[7,8-*h*] quinoline molecule as fascinating as I did when I first discovered it in the literature and while progress has been slow going, with many hurdles along the way, I feel we have made some good progress especially more recently when complexing it with beryllium. Our reported modifications to the original synthesis of the quinolino[7,8-*h*]quinolines now allows for a reliable, multi-gram procedure and thus others that may wish to follow will find the path a little easier to navigate. There have also been some exciting developments with new derivatives by others that will improve solubility and useability.

Acknowledgments

I would like to acknowledge the hard work and persistence of the various PhD students whom I have inflicted aspects of this project on, specifically Drs Karl Shaffer, David Nixon and Rebecca Severinsen.

References

1. Buchner, M.R. *Z. Naturforsch B* **2020**, *75*, 405; Buchner, M.R. *Chem. Commun.* **2020**, *56*, 8895.
2. Taylor, T.P.; Ding, M.; Ehler, D.S.; Foreman, T.M.; Kaszuba, J.P.; Sauer, N.N. *J. Environ. Sci. Health A Toxic/Hazard. Subst. Environ. Eng.* **2003**, *38*, 439.
3. Alder, R.W.; Bowman, P.S.; Steele, W.R.S.; Winterman, D.R. *Chem. Commun.* **1968**, 723–724.
4. Wild, U.; Hübner, O.; Maronna, A.; Enders, M.; Kaifer, E.; Wadepohl, H.; Himmel, H.-J. *Eur. J. Inorg. Chem.* **2008**, 4440–4447.
5. Wüstefeld, H.-U.; Kaska, W.C.; Schüth, F.; Stucky, G.D.; Bu, X.; Krebs, B. *Angew. Chem. Int. Ed.* **2001**, *40*, 3182–3184.
6. Shaffer, K.J.; McLean, T.M.; Waterland, M.R.; Wenzel, M.; Plieger, P.G. *Inorg. Chim. Acta* **2012**, *380*, 278–283.
7. Shaffer, K.J.; Wenzel, M.; Plieger, P.G. *Polyhedron* **2013**, *52*, 1399–1402.
8. Buchanan, J.K.; Severinsen, R.S.; Buchner, M.R.; Thomas-Hargreaves, L.R; Spang, N.; John, K.D; Plieger, P.G. *Dalton Trans.* **2021**, *50*, 16950.
9. Gamage, S.N.; Morris, R.H.; Rettig, S.J.; Thackray, D.C.; Thorburn, I.S.; James, B.R. *J. Chem. Soc. Chem. Commun.* **1987**, 894–895.
10. Yamasaki, T.; Nobutaka, O.; Yasunari, S.; Kozo, O.; Kenji, G.; Fumiko, N.; Masato, H.; Seichi, O. *Chem. Lett.* **2004**, *33*, 928–929.
11. Shaffer, K.S.; Parr, D.C.; Wenzel, M.; Rowlands, G.J.; Plieger, P.G. *Eur. J. Org. Chem.* **2012**, 6967-6975.
12. Rowlands, G.J; Severinsen, R.J.; Buchanan, J. K.; Shaffer, K.J.; Jameson, H.T.; Thennakoon, N.; Leito, I.; Lõkov, M.; Kütt, A.; Vianello, R.; Despotović, I.; Radić, N.; Plieger, P.G. *J. Org. Chem.* **2020**, *85*, 11297-11308.

Article

The versatility of sugar in chemistry education

MARRYLLYN DONALDSON

School of Natural Sciences, Massey University, Palmerston North (Email: m.donaldson@massey.ac.nz)

Keywords: *undergraduate teaching, chemistry education, sugar, home-based experiments*

Introduction

Lolly-based chemistry teaching should occur more often. There are endless ways to incorporate sugar and sweets into experiments to demonstrate fundamental concepts in chemistry. Sugar and lollies provide a means for capturing the student's attention and show them that chemistry is an exciting and relevant part of their everyday lives.

With the pandemic resulting in at-home learning at every level of education, institutes and educators are returning to and developing experiments that can be performed safely with household items that are readily available and no specialised equipment.[1] Some simple examples provided here can be performed at home, while others involve classroom experiments. Sugary treats have been used to teach stoichiometry,[2] atomic orbitals,[3] kinetics, and statistics.[4, 5] From home, the practical side of chemistry can be explored with liquid chromatography,[6] acid/base reactions,[7] combustion,[8] and more.

Table sugar consists of an orderly arrangement of crystalline sucrose molecules. Sucrose is a disaccharide made up of glucose and fructose (Fig. 1). These simple sugars can be linked together in infinite ways. To make most types of lollies, you start by dissolving sugar in boiling water. The variety of lolly making lies in sugar concentration and heating/cooling to manipulate the size and scale of crystallisation or the formation of amorphous, sometimes glassy, states. Varying the techniques and timings of how sugars are heated and cooled produces an array of tastes and textures. Some practical and edible demonstrations of the differing physical conditions can be explored at home and in class.

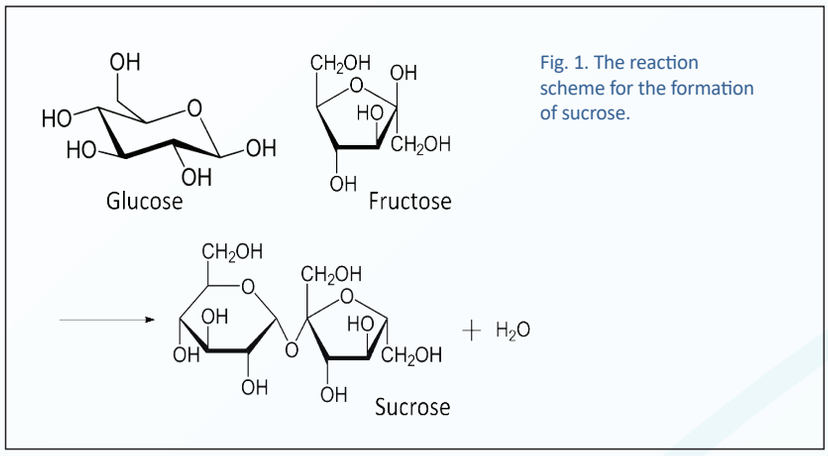

Fig. 1. The reaction scheme for the formation of sucrose.

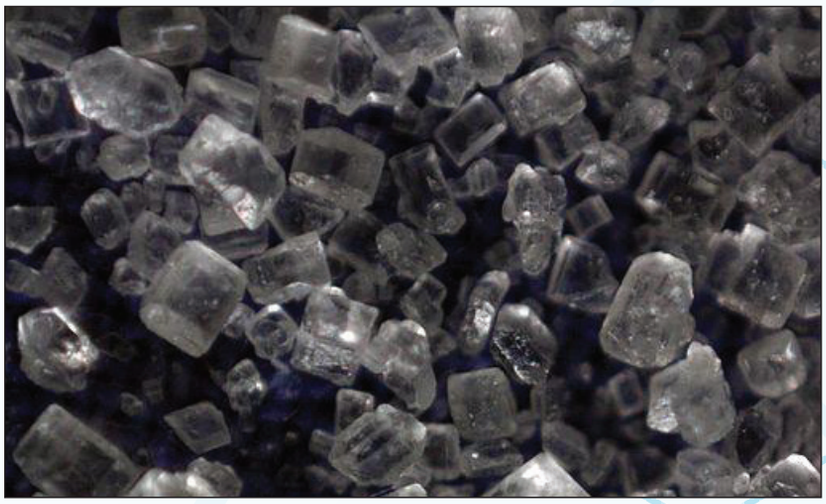

Fig. 2. Sugar crystals. Image courtesy of Edal Anton Leftrov under Creative Commons license CC BY-SA 3.0.10

Sugar crystallisation

The formation of single crystals is vital for preparing materials that provide a wide range of structural information. A simple and delicious way to explore this concept is the slow growth of crystallised sugar rock. Crystals are arrangements of repeating patterns of molecules that extend in all three dimensions. Sugar naturally forms a monoclinic crystal,[9] a pattern of symmetry within the crystal lattice (Fig. 2).

Granulated sugar may have crystalline pieces, but grains of sugar are made up of multiple tiny crystals. A fun introduction to crystals can be to

look at sugar under the microscope and observe their hexagonal pillar arrangement. When crystals are produced quickly, a greater number are grown, resulting in smaller sized crystals overall. Slowing the rate of crystal growth allows for the formation of larger, single, continuous crystals.

Rock crystal lollies

When granulated sugar is dissolved in water, water molecules bind to the sucrose molecules; and pull them away from the crystal and into the solution. Making rock crystals requires a saturated solution of sugar water. At room temperature (25 °C) the solubility of sucrose in water is 210 g/100 mL.[9] The starting solution for this process needs more sugar than can be dissolved in a room temperature system.

When a system is shifted away from equilibrium it acts to restore equilibrium by reacting in opposition to the shift, which is Le Châtelier's principle. An increase in temperature causes the system to decrease energy, in an attempt to bring the temperature down. The breaking of intermolecular chemical bonds absorbs energy, so a greater number of sucrose molecules break apart and dissolve in the solution. The dynamic equilibrium of this sugar system is affected by a change in temperature, whereby heating the solution more sugar is dissolved.[11]

When we cool this supersaturated solution down, the decrease in temperature causes it to release energy through the formation of intermolecular chemical bonds. Hence, crystals form when the temperature decreases.

The slower the temperature, the more molecules join the sugar crystals, and that is how rock candy is created. The slower the temperature of the solution is cooled, the slower molecules are added to a crystal, leading to the growth of larger crystals; with fewer defects. Skewers, or string, dipped in dry sugar are hung in the sugar solution as it cools, acting as a nucleation site (Fig. 3). When left to hang in the solution for a few days, set aside where the reaction vessel won't be disturbed, the skewers will grow large crystals of sugar rock: a portable treat.

"The crystal growth can handle some impurities, so fun can be had by adding some drops of food colouring and flavouring to the bottom of your crystal growth vessel before you add the sugar water. A flavour rainbow of treats can be made."

Fig. 3. Coloured rock crystal lollies growing on skewers

Experimental conditions can be altered to explore how different properties in this experiment can change the outcome. Sugar will only start to crystallise in a supersaturated solution; how does the amount of supersaturation affect crystal growth? How does growth compare when skewers are not pre-dipped with sugar granules, if different types or powdered sugar is used? What if only granules are added as nucleation sites, with no skewer? What results from different initial heating temperatures?[12, 13]

Pure sugar will result in clear crystals, but if there are mineral impurities present, brown crystals form. The crystal growth can handle some impurities, so fun can be had by adding some drops of food colouring and flavouring to the bottom of your crystal growth vessel before you add the sugar water. A flavour rainbow of treats can be made.[14]

Other hard treats

The formation of hard sugar treats is not exclusively done by a slow formation of pure crystals from supersaturation. Other treats, such as peanut brittle or lollipops can be made.

These hard lollies are amorphous like glass. The sugar molecules lack a distinct arrangement in comparison to a crystalline state where molecules are highly organised in a three-dimensional array.

When the sugar syrup is heated to a high enough boiling point (hard-crack stage) the rapid cooling of the supersaturated sugar solution results in a glassy state, with little crystallisation occurring.[15] When solid sugar is heated to a high temperature and rapidly cooled it will reach a glass transition temperature (Tg) where a hard amorphous substance, upon heating, the sugar can become a soft, rubbery material.

Preventing crystal growth can also be done with the introduction of impurities, such as corn-syrup or cream of tartar (tartaric acid). Tartaric acid leads to acid catalysed sucrose hydrolysis, where the sucrose disaccharide breaks down into glucose and fructose, further increasing impurities.

Both techniques can be experimented with to adapt recipes and let students create their own treats.

Fudge

While rock candy is made of large crystals of sugar, other candies, such as fudge, contain smaller sugar crystals.

Obtaining a soft caramel is controlled by a terminal boiling point temperature. A sugar phase diagram can be used to see how different type of sugars are formed (Fig. 4). By heating to 118°C and increasing the sugar concentration, when the system is cooled sufficiently quickly, heterogeneous crystal nucleation is inhibited.[16]

Stirring during the fudge making process also prevents the sugar crystals that start to form from growing too big, by increasing the rate of sucrose molecules meeting. This creates a larger number of crystal seeds and nucleation sites throughout the syrup. The distribution of the sugar molecules into a larger number of crystals results in smaller crystals overall.

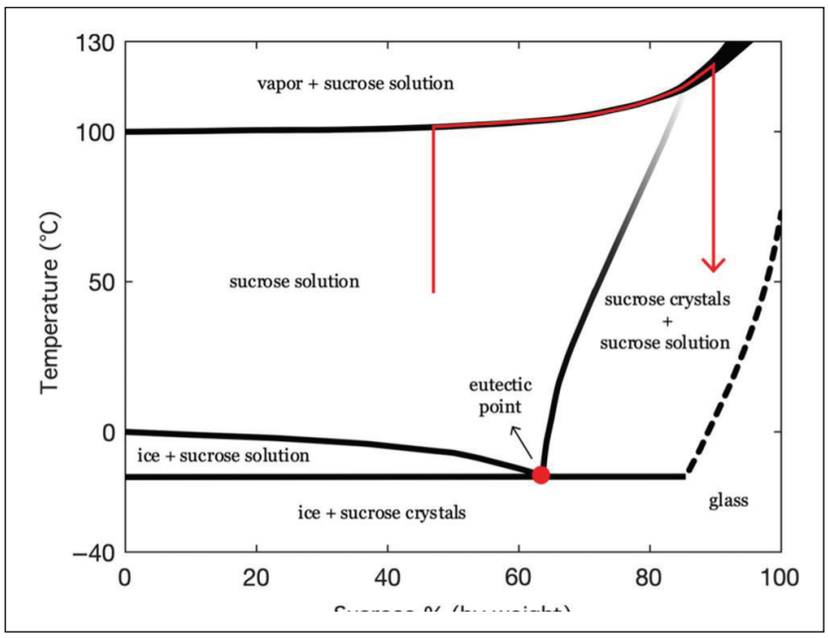

Fig. 4. Sugar phase diagram. Image reproduced with permission of reference 16.

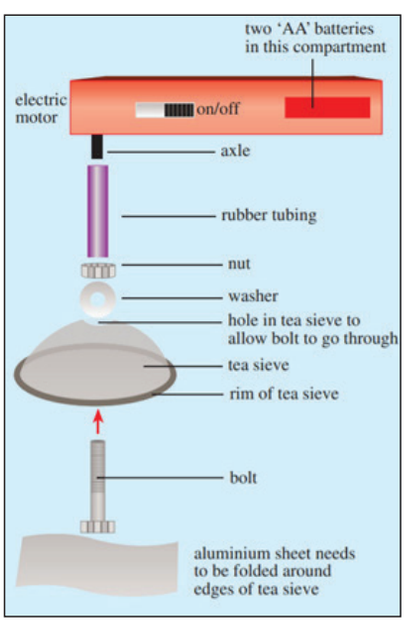

Fig. 5. Above, a student uses a DIY candy floss device, while candy floss is collected on a skewer. Left, Schematic of a homemade candy floss maker. Images reproduced with permission of reference 18.

Candy floss

Candy floss takes the rapid cooling of hot sugar to another level. First, granulated sugar is heated in a cotton candy machine until it melts and the intermolecular forces between the sucrose molecules are broken. The liquefied sugar is then sprayed through tiny nozzles forming filaments of liquid that solidify immediately when exposed to the cooler air around them.[11, 17]

Amir et al. taught a class exploring these physical concepts to put together homemade candy floss makers, to add a 'play factor' (Fig. 5).[18] An open tea sieve closed with an aluminum plate was suspended from the upper part of the tea sieve by a metal bolt and washer. This was attached to a mechanised motor.

Sugar was put on the aluminum plate inside the sieve and the sugar was melted by holding the base of the plate over a Bunsen burner. The device was then held in a high rimmed bowl and the motor was turned on, generating candy floss which can be collected on a skewer.

Exploring physical phenomena

Density

The principles of density and concentration can be explored and discussed by calculating and measuring different concentrations of sugar solutions. When a series of concentrations are mixed with food dyes, they can be carefully layered in a narrow cylinder to produce a layered rainbow solution (Fig. 6).

Alternatively, a more precise analysis of sucrose solution density can be performed. Peterson[19] published a laboratory experiment for measurement of the densities of sugar solutions as a general chemistry experiment for undergraduate students. The lesson plan is included in the supplementary material of the publication.

Lolly chromatography and spectroscopy

Chromatography can be introduced in a wide range of ways. One simple way is extracting the pigments of coloured, sugar-shelled lollies by using salt water to dissolve the coating. The lollies first need to be separated by colour, so that the combinations of pigments for each colour can be investigated.

Thin layer chromatography (TLC) can be performed at home with coffee filter paper that has been cut into rectangles.[21] The extracted samples can then also be analysed using UV-vis spectroscopy,[6] even from home by downloading a colorimeter app on a smartphone.

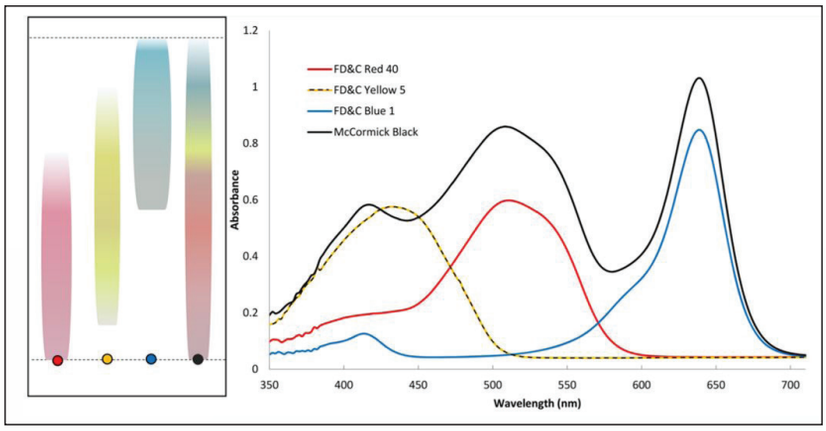

Fig. 7. The outcome of a TLC of food pigment dyes, alongside the resulting UV-vis spectra. Image reproduced with permission of reference 21.

Eq. 1: $2NaHCO_3(s) + heat \rightarrow Na_2CO_3(s) + H_2O(g) + CO_2(g)$

Eq. 2: $NaHCO_3(s) + CH_3COOH(aq) + heat \rightarrow CH_3COONa(aq) + H_2O(g) + CO_2(g)$

Fig. 6. Sugar water rainbow exploring density[20]

Stoichiometry and carbonation

Carbonation in food is readily available to demonstrate reactions that result in gas products.

Hokey pokey

When baking soda (sodium bicarbonate) is heated to a high temperature, it breaks down, giving off carbon dioxide bubbles (Eq. 1) and puffing up the mixture in a dramatic way.[21, 22] Hokey pokey is a New Zealand classic and everyone has their own recipe, and good starter recipes can always be found online.

Students can experiment with the outcomes of the hokey-pokey. The physical structure of the product can be explored; differing amounts of gelatine can be added to the initial sugar mixture to capture larger bubbles of gas and change the final texture. The stoichiometry and gas production can be explored by changing the ratios of baking soda and vinegar (acetic acid) (Eq. 2). This leads to discussions on gas production and how the baking soda and vinegar can affect the final taste.[2]

Fizzy carbonation

There are endless ways of exploring acid/base reactions. One way is to vi-

sually look at the volume of gas given off in a reaction. Pop Rocks are a solid lolly packed with a high density of CO_2 pockets, that result in a pop and fizz in the mouth when dissolved on the tongue.

A simple way of showing this CO_2 release in any classroom is to add Pop Rocks to a carbonated drink and quickly cover the bottle neck with a balloon. The volume of the expanding balloon correlates to the amount of gas given off, and simple graphs can be generated by comparing the mass of Pop Rocks added and the size the balloon expands.[23, 24]

A more specific quantitative analysis can be completed with a titrimetric determination of the carbon dioxide that is released when Pop Rocks are dissolved.[7] Two 250 mL round-bottomed flasks are connected by a three-way distillation head and sealed with a balloon to accommodate the evolving CO_2 gas before it dissolves in solution (Fig.9). Red, orange, yellow or pink balloons should not be used in order to prevent any colour leaching from affecting the results of the phenolphthalein titration results.

For the analysis, three packages (about 30g) of Pop Rocks are put in one flask and 100.00 mL of 0.100 M NaOH in the other. Next, about 100 mL of deionised water is poured onto the Pop Rocks and the distillation head is placed as quickly as possible between the two flasks. The Pop Rocks solution can be stirred overnight or up to a week. A determination of CO_2 can be done by taking a 25 mL aliquot of the NaOH solution and titrating with 0.05 M HCl,[25] first to the phenolphthalein endpoint and then to the methyl orange endpoint.

At the first endpoint sodium carbonate is converted to sodium bicarbonate and the excess sodium hydroxide is consumed. Thus, only sodium bicarbonate (an amount equivalent to the evolved carbon dioxide) was titrated by the HCl as the reaction proceeded to the second endpoint.[7]

Fig. 8. Hokey pokey.

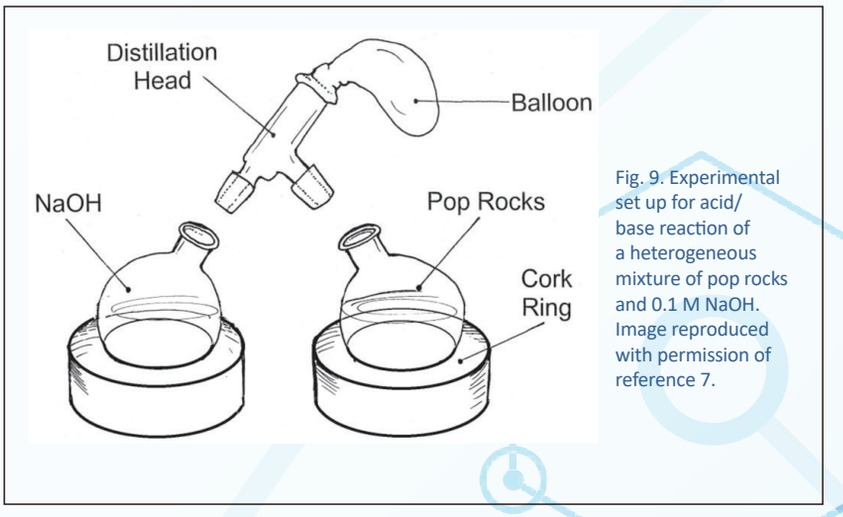

Fig. 9. Experimental set up for acid/base reaction of a heterogeneous mixture of pop rocks and 0.1 M NaOH. Image reproduced with permission of reference 7.

Combustion: sugar rockets

Many different chemicals can be used as rocket fuel, including gunpowder, alcohol and kerosene. Rockets using sugar as the main fuel source demonstrate the highly oxidisable nature of sugar. This experiment can be explored theoretically or as a classroom demonstration.

In this experiment, powdered sugar acts as the fuel and either potassium nitrate or potassium chlorate acts as the oxidiser. These materials need to be finely ground together, melting the sugar but not the KNO_3, so that the KNO_3 grains are fully coated in sugar. Metals must not be used in the process to prevent any premature ignition.[26]

This sugar fuel mix is packed in a plastic or hard card tube and can be sealed with wet kitty litter at both ends. The rocket needs to be perforated with a wooden spike, so that a fuse can be inserted. The rocket can then be mounted on a wooden dowl as a 'launcher', ready to be ignited and launched.

Eqs. 3 & 4 for the combustion of sugar show how a large amount of gas is released upon ignition, which escapes out of the perforation in the base of the rocket, generating propulsion.

Eq. 3: $C_{12}H_{22}O_{11}\,(s) + 8KClO_3\,(s) \rightarrow 8KCl\,(s) + 11H_2O\,(g) + 12CO_2\,(g)$

Eq. 4: $5C_{12}H_{22}O_{11}\,(s) + 48KNO_3\,(s) \rightarrow 24K_2CO_3\,(s) + 24N_2\,(g) + 55H_2O\,(g) + 36CO_2\,(g)$

These sugar rockets were built and used successfully by high school students as an introduction to chemistry by Levine et al.[23] There are various techniques available for building these rockets, noting that appropriate methods suitable for the safety and facilities of each class should be chosen.

More advanced solid rocket motors can not only be throttled but also be extinguished and then re-ignited by controlling the nozzle geometry or through the use of vent ports. Also, pulsed rocket motors that burn in segments and that can be ignited upon command are available. Modern designs may also include a steerable nozzle for guidance, avionics, recovery hardware (parachutes), self-destruct mechanisms, controllable tactical motors, controllable divert and attitude control motors, and thermal management materials.[27]

As an alternative, Eliason *et al.* performed this experiment in a galvanised plumbing pipe with an end cap, in fume hoods, to produce a rocket-like flame that shot out of the tube.[8] This way additives can be added to the fuel to make coloured flames. The amount of colourising salts in the reaction mixture was kept at a constant ratio of 0.2 g salt to 1.0 g reaction mixture, with appropriate mixtures for producing colours shown in Table 1.

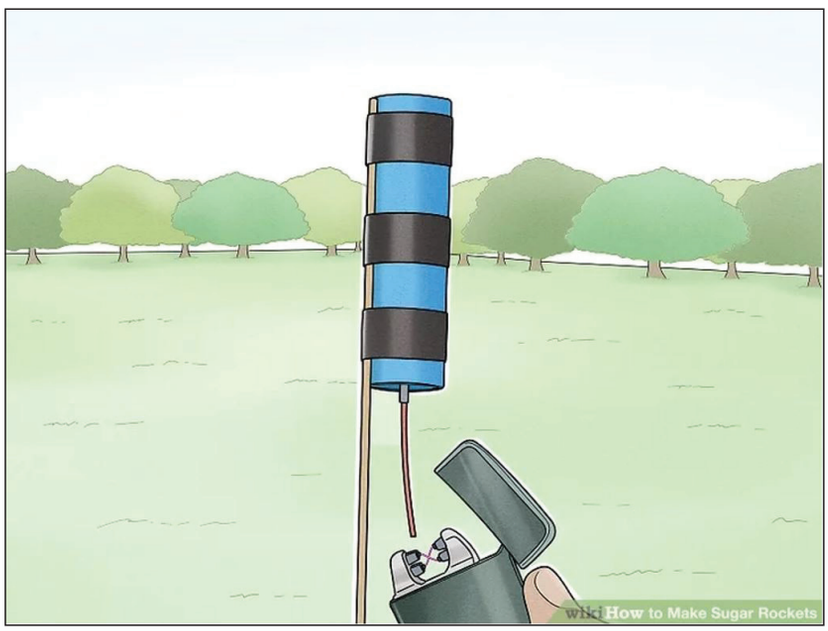

Fig. 10. Wiki-How image for making sugar rockets[28]

Other fun ideas

Another thing sugar and lollies can do in the classroom is to simply act as a physical example for other problems. The simple presence of snacks can make discussing chemistry concepts that little bit more exciting.

Jennings *et al.* used unwrapping and eating chocolate as a demonstration for reaction mechanisms and rate-determining steps.[29] Canaes *et al.* produced a classroom exercise for undergraduate and beginning graduate students to explore both sampling and statistics, using bags of M&Ms as the bulk material that samples are extracted from.[5] Finally, of course, everyone has used lollies on toothpicks to learn about chemical structures.

Conclusions

In summary, sugar-themed science for high-school and undergraduate students can use simple materials to introduce more advanced concepts, with experiments that can be performed at home and in the classroom. Interactive and fun activities can provide hands-on and visual results to demonstrate chemistry's role in the everyday world. Some examples have been explored here, but there are endless other experiments to do.

Colour	
Green	5 g barium chloride, 5 g boric acid, 1 g PVC
Blue	7 g copper(II) chloride, 7 g barium nitrate, 1.5 g PVC
Purple	4.5 g strontium nitrate, 7 g copper(II) chloride, 1 g PVC

Table 1. Additive mixtures that can be added to a sugar fuel to produce coloured flames[8]

References

1. Andrews, J. L.; de Los Rios, J. P.; Rayaluru, M.; Lee, S.; Mai, L.; Schusser, A.; Mak, C. H. *J. Chem. Ed.* **2020,** *97* (7), 1887-1894.
2. Cain, L. *J. Chem. Ed.* **1986,** *63* (12), 1048.
3. Liguori, L. *J. Chem. Ed.* **2014,** *91* (10), 1742-1744.
4. Meloan, M. L.; Meloan, J. M.; Meloan, C. E. *J. Chem. Ed.* **1994,** *71* (8), 658.
5. Canaes, L. S.; Brancalion, M. L.; Rossi, A. V.; Rath, S. *J. Chem. Ed.* **2008,** *85* (8), 1083.
6. Birdwhistell, K. R.; Spence, T. G. *J. Chem. Ed.* **2002,** *79* (7), 847.
7. Davis, C. M.; Mauck, M. C. *J. Chem. Ed.* **2003,** *80* (5), 552.
8. Eliason, R.; Lee, E. J.; Wakefield, D.; Bergren, A. *J. Chem. Ed.* **2000,** *77* (12), 1581.
9. Bubnik, Z.; Kadlec, P. Sucrose solubility. In *Sucrose*, Springer: 1995; pp 101-125.
10. Leftrov, E. A. https://commons.wikimedia.org/wiki/File:Sugar-Crystals-magnified.jpg (accessed 30/01/2022).
11. Husband, T. *ChemMatters* **2014,** *10* (11), 5-8.
12. Bryski, A.; Concepcion, K.; Hashimoto, J.; Patel, S. *The Expedition* **2020,** *11*.
13. Gholamhosseinpour, A.; Varidi, M.; Elahi, M.; Shahidi, F. *Am.-Eurasian J. Agric. Environ. Sci* **2008,** *4* (1), 72-75.
14. Vatankhah Lotfabadi, S.; Mortazavi, S. A.; Yeganehzad, S. *Food Sci. Nutr.* **2020,** *8* (2), 933-941.
15. Šmídová, I.; Čopíková, J.; Maryška, M.; Coimbra, M. A. *Czech J. Food Sci.* **2003,** *21* (5), 185.
16. Altan, I.; Charbonneau, P.; de Valicourt, J. In *Handbook of Molecular Gastronomy*, CRC Press: pp 545-547.
17. Spence, C.; Corujo, A.; Youssef, J. *Int. J. Gastr. Food Sci.* **2019,** *16*, 100146.
18. Amir, N.; Subramaniam, R. *Phys. Ed.* **2009,** *44* (4), 420.
19. Peterson, K. I. *J. Chem. Ed.* **2008,** *85* (8), 1089.
20. https://www.steamsational.com/sugar-rainbow-density-tower/ (accessed 30/01/2022).
21. Bayline, J. L.; Tucci, H. M.; Miller, D. W.; Roderick, K. D.; Brletic, P. A. *J. Chem. Ed.* **2018,** *95* (8), 1307-1315.
22. Mitchell, S. B. *J. Chem. Ed.* **2014,** *91* (10), 1509-1510.
23. Levine, M.; DiScenza, D. J. *J. Chem. Ed.* **2018,** *95* (8), 1316-1322.
24. Coffey, T. *Phys. Teacher* **2008,** *46* (8), 473-476.
25. Crossno, S.; Kalbus, L. H.; Kalbus, G. E. *J. Chem. Ed.* **1996,** *73* (2), 175.
26. Goll, J. G.; Wilkinson, L. J.; Snell, D. M. *J. Chem. Ed.* **2009,** *86* (2), 177.
27. Singh, D. A. *Int. J. Eng. Trends Appl.* **2015,** *2*.
28. https://www.wikihow.com/Make-Sugar-Rockets (accessed 30/01/2022).
29. Jennings, L. D.; Keller, S. W. *J. Chem. Ed.* **2005,** *82* (4), 549.

Article

Towards more energy efficient synthesis of ammonia - a review of photocatalytic nitrogen reduction reactions (NRRs)

AMINU HASSAN YUSUF AND SARAH L. MASTERS*

School of Physical and Chemical Sciences, University of Canterbury, Private Bag 4800, Christchurch 8140 (Email: sarah.masters@canterbury.ac.nz)

Keywords: *ammonia, photocatalysis, nitrogen reduction reaction*

Introduction

The importance of nitrogen to life cannot be overemphasised. It is a key component of various biomolecules such as proteins and nuclei acids, which are the building blocks of life. Despite the abundance of nitrogen in the atmosphere, most life forms on earth cannot effectively utilise nitrogen in the form in which it exists in the atmosphere as N_2.[1] Instead, they get their nitrogen in the form of ammonia or nitrates. This is because the bond dissociation energy in the non-polar triple bond (N≡N, 941 kJ mol^{-1}) is very high, making it unfavourable for N_2 to be cleaved. Nitrogen fixation is the process, either natural or industrial, that causes free nitrogen to combine chemically with other elements to form more-reactive nitrogen compounds such as ammonia (NH_3). Nitrogen fixation occurs geochemically via lightning, biologically through the action of nitrogen fixation by azo-bacteria, and industrially using the Haber-Bosch process.[2] Currently, the bulk of nitrogen fixation is performed industrially. The remaining geological and biological nitrogen fixation only accounts for a small percentage of total nitrogen fixation.[3]

Ammonia is among the world's most popular industrial chemical products with a production of greater than 180 million metric tons per year – more than any other synthetically manufactured chemical in the world.[4] Ammonia is an alkaline, colourless, pungent gas having one nitrogen atom covalently bonded to three hydrogen atoms.[5] Over 80% of the synthesised ammonia is used to produce fertiliser in the form of urea, nitrate, sulfate or bicarbonate[6] for agricultural use. The remaining ammonia is distributed for other applications such as pharmaceutical production, explosives and energy storage.[7,8]

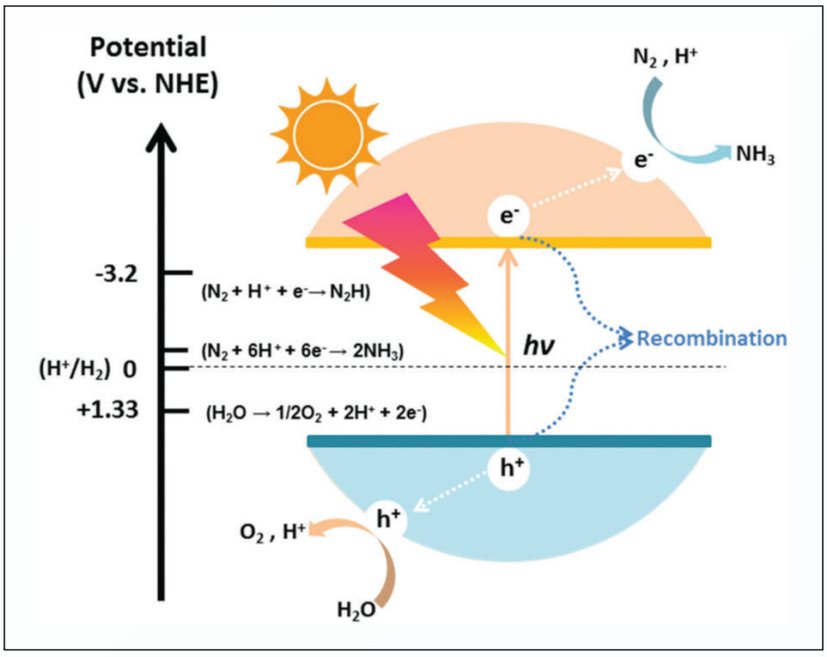

Fig. 1. Schematic of semiconductor-based photocatalysts used for the conversion of N_2 to NH_3. The redox potentials (V vs. NHE at pH = 0) of water splitting and dinitrogen hydrogenation are marked on the left. NHE is the Normal Hydrogen Electrode. Reproduced with permission.[20]

There are three major pathways for conversion of nitrogen into ammonia; azobacter nitrogen decomposition, the Haber-Bosch process and photo/electrocatalytic nitrogen reduction.[9] The conventional Haber-Bosch process has been used for over a century to produce ammonia at very high temperatures (300-500°C) and pressures (150-300 atm) using iron or ruthenium heterogeneous catalysts. This accounts for more than 300 metric tonnes of carbon dioxide emission annually.[10,11] Furthermore, the process requires high capital and infrastructure investment and is responsible for almost 2% of the global fossil energy usage. It also creates serious environmental concerns.[1] Consequently, developing a green, economical and renewable energy-based technology to synthesise ammonia by conversion of nitrogen at ambient conditions is necessary.[12]

Reduction of nitrogen using photochemical and electrochemical processes has great potential for the green synthesis of ammonia, in which the reaction takes place by the addition of protons and electrons derived from solar powered or renewable

resources at ambient conditions.[13] Several photocatalysts have been tested for photocatalytic nitrogen fixation application in the search for an ideal catalyst able to overcome the high-energy barriers to N≡N bond cleavage.[1, 14-16] This review gives an overview of recent developments in the synthesis of efficient photocatalysts for nitrogen reduction reactions (NRRs). Emphasis is placed on design, synthesis and characterisation of efficient photocatalysts for practical application in NRRs.

Principles of photocatalytic nitrogen reduction

Photocatalytic nitrogen fixation is a sustainable process that involves the direct use of solar irradiation for N_2 conversion into ammonia.[17] It is a low temperature and mild pressure reaction that produces far fewer pollutants than industrial methods. In photocatalysis a semiconductor absorbs photons of light to form an electron-hole pair resulting in oxidation and reduction reactions.[18]

Photocatalytic nitrogen reduction is a promising alternative to synthesise NH_3 from N_2 with water as a reducing reagent. The process typically involves oxidation of H_2O to provide protons (Eq. 1) and reduction of N_2 to NH_3 in the presence of photons and a catalyst (Eq. 2), where h^+ is the electron hole.[19]

In photocatalysis, when the semiconductor is illuminated with light energy equal to or greater than the bandgap energy of a photocatalyst, excitation of photogenerated electrons occurs from valence band (VB) to conduction band (CB), leaving behind the photogenerated holes in the VB (Fig. 1). The photogenerated electrons (e^-) and holes (h^+) on the surface of the photocatalyst can either recombine or drive the reduction and oxidation reaction respectively (Fig. 1). Eq. 1 shows the oxidation of water to form H^+ and O_2 by photogenerated holes while Eq. 2 is the reduction half reaction in which the photogenerated electrons are transferred to the adsorbed N_2 molecules, liberating H^+ for the NRR to form NH_3.

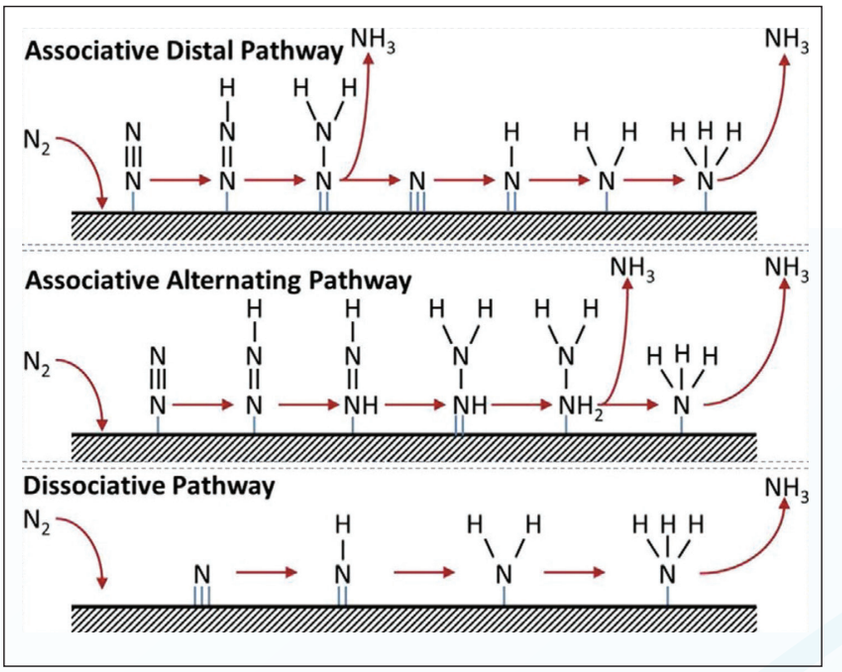

Fig. 2. Associative and dissociative mechanisms of artificial nitrogen fixation. Reproduced with permission.[21]

Eq. 1: $2H_2O + 4h^+ \rightarrow O_2 + 4H^+$

Eq. 2: $N_2 + 6H^+ + 6e^- \rightarrow 2NH_3$

Eq. 3: $2N_2 + 6H_2O \xrightarrow[\text{photocatalyst}]{\text{light}} 4NH_3 + 3O2$

The overall photocalytic process for the formation of NH_3 from H_2O and N_2 on the surface of the photocatalyst under ambient conditions[19] is shown in Eq. 3.

Mechanisms of photocatalytic nitrogen reduction

There are two general mechanisms for the catalytic reduction of nitrogen on a heterogeneous surface; the associative and dissociative mechanisms.[1] The associative mechanism involves consecutive hydrogenation of a dissociated nitrogen molecule to form NH_3.[16] This hydrogenation process proceeds via either an associative distal pathway or an associative alternating pathway. In the associative distal pathway, hydrogen is sequentially added to the nitrogen atom of the N_2 molecule that is not attached to the catalytic surface until the first molecule of NH_3 is generated and released Fig. 2).[21] Then the second nitrogen atom is sequentially protonated to produce the second molecule of NH_3 (Fig. 2a). In the associative alternating pathway, the ammonia production takes place by alternating protonation to both atoms of N_2 before each NH_3 is released (Fig. 2b).[16] The dissociative mechanism involves nitrogen protonation after the N≡N triple bond is cleaved and only a nitrogen atom is attached to the surface (Fig. 2c).

Biological nitrogen decomposition with nitrogenase is generally thought to proceed by the associative mechanism of N_2 molecules[15] while the conventional Haber-Bosch process proceeds by the dissociative mechanism where the nitrogen and hydrogen atoms react after the N_2 triple bond and the H_2 bond are cleaved.

Nitrogen reduction may also proceed via other reaction mechanisms beside the associative and dissociative mechanisms previously discussed.[3] To shed light on this, the various mechanisms of nitrogen reduction can be better understood through the use of theoretical predictions. For this, the reactant(s), product(s) and the pathway between them are predicted using computational methods, usually plane-wave density functional theory (PW-DFT) methods.

There is limited literature available using theoretical methods to predict photocatalytic nitrogen fixation.[22] Most research is focused towards DFT studies for electrocatalytic nitrogen fixation. For example, Xiaolan et al. have theoretically analysed suitable transition metal electrocatalysts in the synthesis of ammonia and the mechanism of the reaction is believed to proceed through associative and dissociative pathways on both flat and stepped Ru (0001) surfaces.[23] The addition of the first electron and proton to N_2 on the flat surface of Ru to produce the $*N_2H$ species is believed to be the rate-determining step in the associative mechanism[1].

Skulason et al. conducted theoretical calculations using DFT for the NRR on ruthenium surfaces and established that dissociation occurs at the ruthenium step and is energetically prohibited on flat terraces.[24] They also found that for the associative mechanism the addition of protons occurs when the N_2 is adsorbed onto the surface of the catalysts followed by the subsequent N≡N bond cleavage until NH_3 is formed, either by the Tafel or Heyrovsky mechanisms. Even though the Heyrovsky mechanism is more favorable, the main difference is that the nitrogen molecule that has been adsorbed can recombine with hydrogen atoms adsorbed previously to form N_2H_x species in following a Tafel mechanism. Electrolytic H atoms can then attach to either the proximal or distal nitrogen atoms directly and are then desorbed to form NH_3 molecules following a Heyrovsky mechanism.[24]

"Ammonia synthesis via photocatalysis using sunlight, nitrogen and water is regarded as an ideal alternative to the Haber-Bosch process as it uses less energy and is more environmentally friendly."

Materials for photocatalytic nitrogen reduction

Ammonia synthesis via photocatalysis using sunlight, nitrogen and water is regarded as an ideal alternative to the Haber-Bosch process as it uses less energy and is more environmentally friendly. Schrauzer and Guth reported ammonia synthesis by artificial photosynthesis using TiO_2 photocatalyst in 1977.[25] Nitrogen reduction has been at the forefront of photocatalysis research particularly in recent years.[25]

Numerous studies on ammonia synthesis using photocatalysis have indicated the use of semiconductor materials including metal oxides (Fe_2O_3, ZnO, WO_3)[26-28] and metal sulfides (CdS, MoS_2, InS_2),[29,30] bismuth-based materials (BiOX, BiO, Bi_2O_3),[29,31,32] carbonaceous materials [graphitic carbon nitrides ($g\text{-}C_3N_4$), graphene oxide (GO)],[33,34] and layered double hydroxides (LDHs).[35] The following sections outline the use of metal oxides and sulfides in more detail before examining the use of metal-free photocatalysts.

Metal oxides

TiO_2, Fe_2O_3 and ZnO have been proposed since the 1940s as potential catalysts for N_2 photoreduction.[36] Although pure TiO_2 does not show activity toward nitrogen reduction, annealing at high temperature induces activity. Rutile has proven activity (at a low over-potential) for photocatalytic nitrogen reduction to ammonia.[37] Density functional calculations were performed by Thiel and co-workers to ascertain the mechanism for NH_3 synthesis through N_2 reduction on the surface of rutile TiO_2 (110) having oxygen vacancies originating from the photolysis of adsorbed water. The reaction was found to be exothermic by ~2.0 eV. An energy barrier (0.4–1.3 eV) was passed by H_2O photolysis at each single step. However, the activity of N_2 reduction on TiO_2 was reported to be very low due to the high strength of the N≡N triple bond.

Several other metal oxide-based materials such as ZnO, BiO, CrO, MnO, FeO, NiO, Cu_2O, VO_2, Cr_2O_3, Ga_2O_3 and Ag_2O have been reported as photocatalyts in place of titanium oxide-based materials for ammonia synthesis via N_2 reduction. They have shown different degrees of activity towards the NRR.[19]

Iron in the form of ferric oxide (Fe_2O_3) was earlier reported as a catalyst for the Haber Bosch process by Dhar and Chowdhry.[36] However, it was found that pure iron is not suitable as a catalyst for the photocatalytic reduction reaction of N_2 unless is it partially reduced[38] or in a hydrous form.[39] Khader et al. reported photoassisted reduction of N_2 with water in the presence of a reduced of ferric oxide (Fe_2O_4) to form NH_3.[40] Unmodified ZnO is also reported to have sufficient activity toward ammonia synthesis under solar irradiation.[27]

Zhou et al. reported the synthesis of preferentially oriented Bi_2WO_6 using the microemulsion and solvothermal method.[22] The reduced metallic

Bi was induced to form a $Bi/BiWO_6$ or Bi/BWO nanodisk simultaneously, due to the reducibility of the ethylene glycol in the solvothermal process. The catalyst orientation enhances the charge separation and prolongs the photoexcited charge carrier lifetimes, thereby increasing the photocatalytic activity of the catalyst toward NH_3 formation. The photocatalyst was tested and the results showed a good N_2 reduction rate of up to 86 µmol g^{-1} h^{-1} under visible light irradiation.

Metal sulfides

Metal sulfides have also recently gained considerable attention for photocatalytic N_2 reduction for ammonia synthesis under visible light. Unlike metal oxides, metal sulfides are mostly employed as composites[41] or multicomponent metal sulfide catalysts such as Zn0.1Sn0.1Cd0.8S[42] and Mo0.1Ni0.1Cd0.8S.[43] Nevertheless, Sun et al. (2017) reported high efficient single atom electron-rich MoS_2 with sulfur vacancies.[30] The photocatalytic activity of the catalyst was linked to the formation of electrons and a hole, which allows the transfer of six electrons simultaneously. Zhao et al. also reported the photocatalytic synthesis of NH_3 using ultrathin MoS_2 as a photocatalyst with a rate of up to 325 µmolg^{-1} h^{-1}.[44]

Several studies on photocatalytic activity of different composites of CdS such as CdS/Pt,[45] $CdS/Pt/RuO_2$[27] and $Pt/CdSAg_2S/RuO_2$[46] have suggested higher NH_3 yield than that of pristine CdS under UV light irradiation.

Xing et al. investigated the photocatalytic performance of the MoS_2/C-ZnO composite under irradiation with simulated sunlight and a high performance of N_2 reduction to ammonia was recorded.[41] The result was linked to an efficient charge separation and large surface area of the photocatalyst. Gao et al. also used a NiS/CdS co-catalyst and synthesised NH_3 through the N_2 reduction reaction using photocatalysis.[29] Temperature-programmed desorption confirmed that N_2 molecules adsorb preferentially onto the co-catalyst surface (NiS/CdS), and that the overpotential of the N_2 reduction process decreases on NiS loading.

"Similarly to metal sulfides, non-metal photocatalysts are mostly employed in combination with two or more compounds acting as a co-catalyst in a multicomponent or in the form of a heterojunction with other semiconductors."

Metal-free materials

Recently, photocatalytic nitrogen conversion to ammonia using metal-free materials has gained a lot of attention especially using carbonaceous material such as carbon nitrides and other non-metallic compounds. Similarly to metal sulfides, non-metal photocatalysts are mostly employed in combination with two or more compounds acting as a co-catalyst in a multicomponent or in the form of a heterojunction with other semiconductors.

Waikang et al. reported the synthesis of cyano-group-modified g-C_3N_4 nanoribbon (mCNN) photocatalyst with an enhanced capability towards NH_3 synthesis (a rate of 3.42 µmol g^{-1} h^{-1}) under visible light irradiation.[33] To further understand the involvement of cyano groups in the photocatalytic reaction process, a mCNN model photocatalyst was used to identify the reaction mechanism on the C≡N triple bond active sites. The study confirmed a different pathway for the C≡N triple bond replacement analogous to the Mars van Krevelen (MvK) mechanism by formation of N-K bond in mCNN as proved by DFT calculation[33]

Jin et al. prepared a N-deficient C_3N_4 photocatalyst for the photocatalytic N_2 conversion into ammonia through a dielectric barrier discharge plasma treatment.[47] They found that N vacancies on the photocatalyst act as chemical adsorption sites for the activation of nitrogen. A two-pathway mechanism for the synthesis of ammonia was proposed, in which H_2O_2 is included when air was used as the reaction gas instead of N_2.[16]

Photocatalyst performance

Different methods have been employed to enhance the photocatalytic response of nitrogen reaction through modification of photophysical and surface properties on the photocatalyst or by combination of both. Strategies include the introduction of surface defects,[48] doping,[49] addition of co-catalysts[50] and formation of heterojunctions.[8]

Band gap energy of the semiconductor

The ideal band gap for the photocatalytic nitrogen reaction is close to 2.0 eV with wavelengths of light up to 620 nm. The value of the CB should be less than the overpotential of N_2 (-0.092 V vs. NHE) and VB must be greater than the oxidation potential of water (1.23 V vs. NHE) for the photocatalytic process to occur.[49] Most photocatalysts suffer inadequate visible light response due to the band gap being too narrow or too wide,[48] and as such the photocatalyst has to be made suitable for photocatalytic reaction through surface modification.

Qin et al. reported the synthesis of the heterostructure photocatalyst AT-30 from combination of $AgInS_2$ nanoparticles and 2D MXene (Ti_3C_2) nanosheets. $AgInS_2$ and Ti_3C_2 have band gaps of 1.62 eV (wide) and 0.75 eV (small) respectively.[51] The new heterostructure formed has an

efficient band gap to participate in the photocatalytic NRR and the ammonia yield is believed to be of the order 38.8 μmol g^{-1} h^{-1}.

Doping with either metals or non-metallic compounds has also proven to be a very effective method to alter the band gap of semiconductor photocatalysts to an appropriate energy for NRR. Among metallic dopants, iron has been extensively researched, particularly for TiO_2 photocatalytic materials. Augugliaro et al. reported improved NH_3 yields from photocatalytic N_2 reduction using Fe_2O_3-hybridised TiO_2 on Al_2O_3 as a photocatalyst.[52] Likewise, some non-metallic atoms have also been used to enhance the band gap of a photocatalyst for efficient NH_3 synthesis. For example, a flower-like N-doped MoS_2 (N-MoS_2) was prepared using solvothermal methods.[53] Results confirmed that the N-doping narrowed the band gap and shifted the photo response of the photocatalyst for visible light utilisation resulting in successful photoreduction of N_2 to NH_3 on the surface of N-MoS_2. The rate of ammonia production was found to increase to 121.2 μmol g^{-1} h^{-1}.[53]

In addition to the strategies outlined above, reducing the thickness of the crystal for the photocatalyst has also been used to improve the band gap of semiconductor materials. For instance, Xue and coworkers used a simple molecular self-assembly method to prepare a parous few-layer g-C_3N_4.[54] Contrary to the original g-C_3N_4, the prepared material is ultra-thin in nature. The band gap energy was reduced from 2.69 eV to 2.61 eV, allowing proper utilisation of visible light.

Efficiency of charge separation

Increasing surface defects such as oxygen vacancies is a common method to enhance the efficiency of charge separation in photocatalysts.

"It is extremely important to understand the nature of the active site in the photocatalytic reaction to be able to improve the activity. However, current research does not really focus on understanding the active site on the catalyst."

Approaches such as doping, heterojunction construction and using a co-catalyst are the easiest means for achieving effective charge separation of a photocatalyst for the NRR.

Transition metal dopants have been shown to improve charge separation for photocatalytic nitrogen reduction yet some were found to hinder the process because the active site of the TiO_2 photocatalytic material was covered by their particles thus changing the surface defects.[55] Schrauzer and Guth investigated some transition metals dopants such as Co, Mo, Ni, Pd, V, Cr, Cu, Pt, Ag, Au and Pb and found that only Co, Mo, and Ni dopants improved the NH_3 yields.[25]

A co-catalyst has also been used as a promoter to enhance the electron transfer efficiency of the photocatalyst material. Qiu reported the use of black phosphorus as a co-catalyst of graphite carbon nitride (g-C_3N_4).[56] The introduction of the co-catalyst is found to increase the efficiency of separation charge carriers by forming covalent bonds between carbon and nitrogen and increasing the number of excited electrons.

The use of a heterojunction to enhance the charge transfer ability of the photocatalyst has also been reported as an efficient means to improve the NH_3 yield. Chen et al. described the construction of a Z-scheme type heterojunction of AgBr and $Bi_4O_5Br_2$ to improve the photocatalytic performance of N_2 under visible light, finding that AgBr decomposed and acted as a charge transfer bridge.[57]

Chemical adsorption of nitrogen

Many photocatalysts have difficulties adsorbing enough N_2 due to the surface being too small[58] or smooth[59] resulting in low photocatalytic efficiency. To efficiently improve the N_2 adsorption on the photocatalyst surface for effective nitrogen reduction under visible light irradiation, the roughness of the material is increased by chemical exfoliation, which directly improves the specific surface area and promotes nitrogen adsorption of the material.

Synthesis of edge-rich black phosphorus nanoflakes (eBP NFs) through a chemical etching exfoliation method was reported by Bian and coworkers.[60] The eBP NFs was reported to have a rough surface and rich edges allowing a significant amount of N_2 to be adsorbed on the edge of the material. The photocatalytic activity of the material toward NH_3 production was reported as being sufficient. Zhang et al. also reported the synthesis of ultra-thin carbon nitride (g-C_3N_4-V) using a high-temperature peeling method. [61] Here the carbon vacancies are found to have a direct influence in activating and improving the adsorption of N_2 as well as increasing the photocatalytic activity of the photocatalyst material. However, it is worth noting that an increase in active sites plays a more important role in increasing the chemical adsorption sites than specific surface area. Ammonia desorption also plays a significant role in photocatalytic nitrogen reduction.[62]

Availability of active sites

The availability of active sites on the photocatalyst surface is very important in catalytic reactions as it provides an effective means for

the transfer of photoexcited carriers from the catalyst to adsorbed N_2 molecules.[63] The commonest active sites are vacancies (O, N and others)[64] generated by the catalyst itself and foreign elements (mostly as metallic dopants).[65,66] A vacancy is a surface defect that can be found to be an active site of the material. Oxygen and nitrogen vacancies are commonest in photocatalytic reactions and both occur after oxygen and nitrogen break away in the crystal lattice of oxygen and nitrogen containing compounds respectively.[67]

Fan et al. prepared an oxygen vacancy-induced $In(OH)_3$/carbon nitride (OV-$In(OH)_3$/CN). [68] It was confirmed that $In(OH)_3$ in the heterojunction is rich in oxygen vacancies. Even though the photogenerated electrons cannot be generated under visible light, excited electrons can be captured in g-C_3N_4, thus improving the charge separation efficiency by chemically adsorbing more N_2.

Xue et al. also reported the synthesis of modified g-C_3N_4 by alkali treatment with 7.6 times more activity than the original g-C_3N_4 towards nitrogen fixation. [63] Xue and coworkers used urea-assisted heat treatment to prepare a porous NC-g-C_3N_4 with nitrogen defects and cyano groups. Treatment with an alkaline solution by etching breaks the H-bond in the material, thereby accelerating the thermal polymerisation of urea and subsequent formation of nitrogen vacancies.

In addition to oxygen and nitrogen vacancies, several others such carbon, iodine, sulfur and fluorine have been identified.[61] Similar to O and N, these vacancies also act as a reaction centre to adsorb and activate N_2 as well as enhance the separation of photogenerated carriers.

It is extremely important to understand the nature of the active site in the photocatalytic reaction to be able to improve the activity. However, current research does not really focus on understanding the active site on the catalyst. Computational methods such as density functional theory (DFT) are occasionally used to predict the nature of the active site but the nitrogen absorption-desorption isotherm, temperature programmed desorption of N_2 and in situ FTIR spectroscopy are also more frequently used to indirectly prove the existence of an active site.[15]

"Current research aims to find efficient photo/electrocatalysts for nitrogen reduction under ambient conditions as a sustainable way to synthesise ammonia."

Computational methods

Although research has focused more on the computational study of the NRR using electrocatalysis, there are some reports of the use of DFT to study photocatalytic nitrogen reduction. DFT predicts the mechanisms of the process, the nature of the active site, general properties and the activity as well as the selectivity of the photocatalysts towards nitrogen reduction and other competing reactions.

Casey-Stevens et al. used DFT in conjunction with the Vienna ab initio Simulation Package (VASP) to predict the activation barriers for N_2 dissociation at different active sites of a Ru nanoparticle step (edge and planar sites).[69] The selected sites are based on the hexagonal close-packed (hcp; 0001 and 1011) surfaces present on a Ru NP. The selected sites also considered an edge that was generally assumed to be inactive and sites previously studied for N_2 dissociation.[70] The Bayesian error estimation functional with van der Waals correlation (BEEF-vdW) functional approximation was used and valence electrons were represented on a plane-wave basis with an energy cutoff of 400 eV and a Monkhorst-Pack k-point sampling of 6 x 2 x 1 was used for all surfaces. The projector-augmented wave (PAW) data sets were used to represent ionic cores. The self-consistent electron density was determined by iterative diagonalisation of the Kohn-Sham Hamiltonian according to a Fermi-Dirac distribution with a smearing parameter of kBT = 0.1 eV. It was revealed that the five-fold ruthenium atom active site geometry leads to the most active site for N_2 dissociation as reported previously.[70] However, it was observed that the active site of the four-fold ruthenium atom geometry also offers sufficient stabilization for N_2 dissociation barriers on some edge and planar sites.

Lv et al. also use DFT and a computational hydrogen electrode (CHE) to rationally design and explore the stability of B@g-CN [a single B atom supported on holey graphitic carbon nitride (g-CN)] towards the NRR. All spin-polarised first-principles DFT calculations were performed using VASP.[71] The PAW potentials were adopted with the generalised gradient approximation (GGA) using the Perdew–Burke-Ernzerhof (PBE) exchange-correlation function. A corrected DFT-D2 was also used to account for the van der Waals interactions.

The cutoff energy for the plane wave basis was set to 500 eV, and the convergence criteria for residual force and energy were set to 0.01 eV/Å and 10^{-5} eV, respectively. A g-CN was sampled at 5 x 5 x 1 and 11 x 11 x 1 k-point meshes for structure optimisation and electronic property calculations, respectively. The results confirms that a σ donation – π* back donation plays an important role in the capture and activation of N_2. In addition, the selectivity of B@g-CN towards the NRR is favored over the competing hydrogen evolution reaction (HER) driven by the photogen-

erated electrons from the material. NRRs also occur through the enzymatic pathway with a quite low overpotential of 0.15 V and activation barrier of 0.61 eV.[71]

Wan and coworkers also used DFT to screen the ideal transition metal nitrate (TMN_4) embedded graphene catalysts that exhibited the appropriate catalytic activity for nitrogen reduction into ammonia.[72] Again VASP was used and the PAW method adopted to describe the ion-electron interactions. The electron exchange-correlation was described using PBE.

A cutoff energy of 450 eV was set and 3 x 3 x 1 Gamma center Monkhorst-Pack meshes were used for sampling. The results revealed that among the screened TMN_4 (TM = Fe, Co, Mo, W, Ru and Rh), the MoN_4 model showed the desired catalytic activation toward the NRR. MoN_4 has both occupied and unoccupied d-orbitals which is a very significant factor for nitrogen reduction to ammonia. Bader charge analysis also confirmed that the graphene acted as an electron reservoir and TMN_4 was the electron transmitter and the active site for the reduction process.[72]

Johnson et al. also reported the use of DFT to study a group of MXenes with and without functional groups (M_2XT_x; M= Ti, V, Zr, Nb, Mo, Ta, W; X = C, N; T_x= S, F, Cl) for catalytic activity in the NRR.[73] Unlike previously, the calculation was performed using the Quantum Espresso software package and Ultrasoft Vanderbilt pseudopotentials were employed at plane wave energy of 700 eV. The BEEF-vdW electron exchange correlation was adopted as previously used to model Mxene.[74] The results support previous findings that bare Mxenes of Mo_2C, Mo_2N, W_2C and W_2N are suitable for NRR through an associative mechanism but, based on a combination of stability and selectivity analysis with respect to the competing HER, not all Mxenes are suitable for NRR. The H-terminated Mxenes W_2CH_2 are the only ones found to be suitable for NRR on the basis of thermodynamic analysis.[73]

"Recent developments in decarbonising heavy industries, including shipping, aviation, heat and power generation and chemical production by Natali and co-workers have led to a breakthrough in new technology called liquium."

Conclusions and outlook

Current research aims to find efficient photo/electrocatalysts for nitrogen reduction under ambient conditions as a sustainable way to synthesise ammonia. However, efforts have mainly been focused on metal-based catalysts, especially the transition metals, supported by various two-dimensional materials such as graphene,[75-77] MoS_2,[78-80] BN[81] and g-C_3N_4[82] that give unique electronic and optical properties. Transition metals have proven to be good candidates for the NRR due to the presence of both empty and occupied d-orbitals that can accept / donate electrons to N_2, weakening the N≡N triple bond.[83] However, challenges still remain, such as high cost, low selectivity, poor durability and environmental pollution due to unwanted side reactions.[84] Therefore, developing low cost, eco-friendly metal-free catalysts with a desirable performance has become necessary.

Although the metal-free catalysts for NRRs are of great economic and scientific importance due to their low cost, availability and sustainability,[3] they are still rarely explored as compared to metal-based catalysts even though their properties show great potential in photo/electrocatalytic N_2 fixation.[85] The majority of the research to date has focused on carbon-based metal-free materials such graphene, carbon nanotubes and other carbonaceous material such g-C_3N_4 owing to their availability, stability and unique surface properties.[86] Recently, new 2D metal-free catalysts have emerged, including black phosphorus,[87] boron nitride[86] and carbide,[88] with good electrical and optical properties. These have been used in various applications including photo/electrocatalytic nitrogen fixation.

Recent developments in decarbonising heavy industries, including shipping, aviation, heat and power generation and chemical production by Natali and co-workers have led to a breakthrough in new technology called liquium.[89] This has the potential to revolutionise the production of ammonia at scale by using rare earth or earth nitride materials, lowering the temperature required and utilising atmospheric conditions thereby significantly reducing carbon dioxide emissions.[90] The technology has proven to be economically viable and environmentally friendly and can produce up to 3000 tons/day of ammonia.[89]

It is clear that there is still a plethora of materials to be investigated both computationally and experimentally to continue the push towards more sustainable synthesis of ammonia.

References

1. Lee, J.; Tan, L.-L.; Chai, S.-P. *Nanoscale* **2021**, 24-31.
2. Marakatti, V. S.; Gaigneaux, E. M. *ChemCatChem* **2020,** *17*, 18-63.
3. Guo, C.; Ran, J.; Vasileff, A.; Qiao, S.-Z. *Energy Environ. Sci.* **2018,** *11*(1), 45-56.
4. Terando, A.; Reidmiller, D.; Hostetler, S. W.; Littell, J. S.; Beard Jr, T. D.; Weiskopf, S. R.; Belnap, J.; Plumlee, G. S. *US Department of the Interior, US Geological Survey: 2020*.
5. Upadhyay, D.; Roondhe, B.; Pratap, A.; Jha, P. K. *Appl. Surf. Sci.* **2019**, *476*, 198-204.
6. Foster, S. L.; Bakovic, S. I. P.; Duda, R. D.; Maheshwari, S.; Milton, R. D.; Minteer, S. D.; Janik, M. J.; Renner, J. N.; Greenlee, L. F. *Nat. Catal.* **2018,** *1*(7), 490-500.
7. He, Z.; Wang, Y.; Dong, X.; Zheng, N.; Ma, H.; Zhang, X. *RSC Adv.* **2019,** *9*(38), 21646-21652.
8. Tong, N.; Wang, Y.; Liu, Y.; Li, M.; Zhang, Z.; Huang, H.; Sun, T.; Yang, J.; Li, F.; Wang, X. *J. Catal.* **2018,** *361*, 303-312.
9. Guo, X.; Du, H.; Qu, F.; Li, J. *J. Mater. Chem. A* **2019,** *7*(8), 3531-3543.
10. Mukherjee, A.; Milstein, D. *ACS Catal.* **2018,** *8*(12), 11435-11469.
11. Chirik, P. J. *Nat. Chem.* **2009,** *1*(7), 520-522.
12. Zheng, G.; Yan, J. M.; Yu, G. *Small Methods* **2019,** *3*(6), 1900070-1900073.
13. Kitano, M.; Kujirai, J.; Ogasawara, K.; Matsuishi, S.; Tada, T.; Abe, H.; Niwa, Y.; Hosono, H. *J. Am. Chem. Soc.* **2019,** *141*(51), 20344-20353.
14. Cheng, M.; Xiao, C.; Xie, Y. *J. Mater. Chem. A* **2019,** *7*(34), 19616-19633.
15. Li, M.; Huang, H.; Low, J.; Gao, C.; Long, R.; Xiong, Y. *Small Methods* **2019,** *3*(6), 1800388-1800405
16. He, C.; Wang, J.; Fu, L.; Zhao, C.; Huo, J. *Chin. Chem. Lett.* **2021,** corrected online proof: https://www.sciencedirect.com/science/article/pii/S100184172100721X (accessed 06/12/2021).
17. Wang, H.; He, W.; Wang, H.; Dong, F. *Sci. Bull.* **2018,** *63*(2), 117-125.
18. Huang, R.; Li, X.; Gao, W.; Zhang, X.; Liang, S.; Luo, M., *RSC Adv.* **2021,** *11*(24), 14844-14861.
19. Yang, J.; Li, D.; Zhang, Z.; Li, Q.; Wang, H. *J. Photochem. Photobiol. A* **2000,** *137*(2-3), 197-202.
20. Chen, X.; Li, N.; Kong, Z.; Ong, W.-J.; Zhao, X. *Mater. Horiz.* **2018,** *5*(1), 9-27.
21. Shipman, M. A.; Symes, M. D. *Catal. Today* **2017,** *286*, 57-68.
22. Zhou, S.; Zhang, C.; Liu, J.; Liao, J.; Kong, Y.; Xu, Y.; Chen, G. *Catal. Sci. Technol.* **2019,** *9*(20), 5562-5566.
23. Xue, X.; Chen, R.; Yan, C.; Zhao, P.; Hu, Y.; Zhang, W.; Yang, S.; Jin, Z. *Nano Res.* **2019,** *12*(6), 1229-1249.
24. Skulason, E.; Bligaard, T.; Gudmundsdóttir, S.; Studt, F.; Rossmeisl, J.; Abild-Pedersen, F.; Vegge, T.; Jónsson, H.; Nørskov, J. K. *Phys. Chem. Chem. Phys.* **2012,** *14*(3), 1235-1245.
25. Schrauzer, G.; Guth, T. *J. Am. Chem. Soc.* **1977,** *99*(22), 7189-7193.
26. Lashgari, M.; Zeinalkhani, P. *Appl. Catal. A: Gen.* **2017,** *529*, 91-97.
27. Janet, C.; Navaladian, S.; Viswanathan, B.; Varadarajan, T.; Viswanath, R. *J. Phys. Chem. C* **2010,** *114*(6), 2622-2632.
28. Endoh, E.; Leland, J. K.; Bard, A. J. *J. Phys. Chem.* **1986,** *90*(23), 6223-6226.
29. Gao, X.; An, L.; Qu, D.; Jiang, W.; Chai, Y.; Sun, S.; Liu, X.; Sun, Z. *Sci. Bull.* **2019,** *64*(13), 918-925.
30. Sun, S.; Li, X.; Wang, W.; Zhang, L.; Sun, X. *Appl. Catal. B: Env.* **2017,** *200*, 323-329.
31. Liang, C.; Niu, H.-Y.; Guo, H.; Niu, C.-G.; Yang, Y.-Y.; Liu, H.-Y.; Tang, W.-W.; Feng, H.-P. *Chem. Eng. J.* **2021,** *406*, 126868.
32. Bi, Y.; Wang, Y.; Dong, X.; Zheng, N.; Ma, H.; Zhang, X. *RSC Adv.* **2018,** *8*(39), 21871-21878.
33. Wang, W.; Zhang, H.; Zhang, S.; Liu, Y.; Wang, G.; Sun, C.; Zhao, H. *Angew. Chem. Int. Ed.* **2019,** *58*(46), 16644-16650.
34. Dong, G.; Ho, W.; Wang, C. *J. Mater. Chem. A* **2015,** *3*(46), 23435-23441.
35. Zhao, Y.; Waterhouse, G. I.; Chen, G.; Xiong, X.; Wu, L.-Z.; Tung, C.-H.; Zhang, T. *Chem. Soc. Rev.* **2019,** *48*(7), 1972-2010.
36. Dhar, N.; Pant, N. *Nature* **1944,** *153*(3873), 115-116.
37. Wu, S.; Tan, X.; Liu, K.; Lei, J.; Wang, L.; Zhang, J. *Catal. Today* **2019,** *335*, 214-220.
38. Liu, Q.; Ai, L.; Jiang, J. *J. Mater. Chem. A* **2018,** *6*(9), 4102-4110.
39. Linnik, O. P.; Kisch, H. *Mendeleev Commun.* **2008,** *1*(18), 10-11.
40. Khader, M. M.; Lichtin, N. N.; Vurens, G. H.; Salmeron, M.; Somorjai, G. A. *Langmuir* **1987,** *3*(2), 303-304.
41. Xing, M.; Xu, W.; Dong, C.; Bai, Y.; Zeng, J.; Zhou, Y.; Zhang, J.; Yin, Y. *Chem* **2018,** *4*(6), 1359-1372.
42. Tennakone, K.; Punchihewa, S.; Tantrigoda, R. *Sol. Energy Mater.* **1989,** *18*(3-4), 217-221.
43. Li, Q.-S.; Domen, K.; Naito, S.; Onishi, T.; Tamaru, K. *Chem. Lett.* **1983,** *12*(3), 321-324.
44. Zhao, L., Hadlocon L. S. *Agric. Eng. Int.: CIGR J.* **2015,** Special Issue, 41-51
45. Miyama, H.; Fujii, N.; Nagae, Y. *Chem. Phys. Lett.* **1980,** *74*(3), 523-524.
46. Tennakone, K.; Ileperuma, O.; Thaminimulla, C.; Bandara, J. *J. Photochem. Photobiol. A* **1992,** *66*(3), 375-378.
47. Jin, H.; Liu, X.; Jiao, Y.; Vasileff, A.; Zheng, Y.; Qiao, S.-Z. *Nano Energy* **2018,** *53*, 690-697.
48. Hu, S.; Chen, X.; Li, Q.; Li, F.; Fan, Z.; Wang, H.; Wang, Y.; Zheng, B.; Wu, G. *Appl. Catal. B: Env.* **2017,** *201*, 58-69.
49. Zhang, N.; Jalil, A.; Wu, D.; Chen, S.; Liu, Y.; Gao, C.; Ye, W.; Qi, Z.; Ju, H.; Wang, C.; Wu, X.; Song, L.; Zhu, J.; Xiong, Y. *J. Am. Chem. Soc.* **2018,** *140*(30), 9434-9443.
50. Ye, L.; Han, C.; Ma, Z.; Leng, Y.; Li, J.; Ji, X.; Bi, D.; Xie, H.; Huang, Z. *Chem. Eng. J.* **2017,** *307*, 311-318.
51. Qin, J.; Hu, X.; Li, X.; Yin, Z.; Liu, B.; Lam, K.-h. *Nano Energy* **2019,** *61*, 27-35.
52. Augugliaro, V.; Lauricella, A.; Rizzuti, L.; Schiavello, M.; Sclafani, A. *Int. J. Hydrog. Energy* **1982,** *7*(11), 845-849.
53. Maimaitizi, H.; Abulizi, A.; Zhang, T.; Okitsu, K.; Zhu, J.-J. *Ultrason. Sonochem.* **2020,** *63*, 104956-104966
54. Xue, Y.; Kong, X.; Guo, Y.; Liang, Z.; Cui, H.; Tian, J. *J. Materiomics* **2020,** *6*(1), 128-137.

55. Hirakawa, H.; Hashimoto, M.; Shiraishi, Y.; Hirai, T. *J. Am. Chem. Soc.* **2017,** *139*(31), 10929-10936.

56. Qiu, P.; Xu, C.; Zhou, N.; Chen, H.; Jiang, F. *Appl. Catal. B: Env.* **2018,** *221*, 27-35.

57. Chen, Y.; Zhao, C.; Ma, S.; Xing, P.; Hu, X.; Wu, Y.; He, Y. *Inorg. Chem. Front.* **2019,** *6*(11), 3083-3092.

58. Wang, H.; Zhao, R.; Qin, J.; Hu, H.; Fan, X.; Cao, X.; Wang, D. *ACS Appl. Mater. Interfaces* **2019,** *11*(47), 44249-44262.

59. Chen, W.; Li, X.-H.; He, P.; Wang, T.; Zhang, X.-W.; Li, Y.-G. *ChemSusChem.* **2020**, *11*(10), 27692778.

60. Bian, S.; Wen, M.; Wang, J.; Yang, N.; Chu, P. K.; Yu, X.-F. *J. Phys. Chem. Lett.* **2020,** *11*(3), 1052-1058.

61. Zhang, Y.; Di, J.; Ding, P.; Zhao, J.; Gu, K.; Chen, X.; Yan, C.; Yin, S.; Xia, J.; Li, H. *J. Colloid Interface Sci.* **2019,** *553*, 530-539.

62. Gao, W.; Li, X.; Luo, S.; Luo, Z.; Zhang, X.; Huang, R.; Luo, M. *J. Colloid Interface Sci.* **2021,** *585*, 20-29.

63. Xue, Y.; Guo, Y.; Liang, Z.; Cui, H.; Tian, J. *J. Colloid Interface Sci.* **2019,** *556*, 206-213.

64. Li, J.; Li, H.; Zhan, G.; Zhang, L. *Acc. Chem. Res.* **2017,** *50*(1), 112-121.

65. Wang, S.; Wei, W.; Lv, X.; Huang, B.; Dai, Y. *J. Mater. Chem. A* **2020,** *8*(3), 1378-1385.

66. Xiao, C.; Wang, H.; Zhang, L.; Sun, S.; Wang, W. *ChemCatChem.* **2019,** *11*(24), 6467-6472.

67. Li, S. J.; Bao, D.; Shi, M. M.; Wulan, B. R.; Yan, J. M.; Jiang, Q. *Adv. Mater.* **2017,** *29*(33), 1700001-1700008.

68. Fan, J.; Zuo, M.; Ding, Z.; Zhao, Z.; Liu, J.; Sun, B. *Chem. Eng. J.* **2020,** *396*, 125263-125273

69. Casey-Stevens, C. A.; Lambie, S. G.; Ruffman, C.; Skúlason, E.; Garden, A. L. *J. Phys. Chem. C* **2019,** *123*(50), 30458-30466.

70. Gavnholt, J.; Schiøtz, J. *Phys. Rev. B* **2008,** *77*(3), 035404.

71. Lv, X.; Wei, W.; Li, F.; Huang, B.; Dai, Y. *Nano letters* **2019,** *19*(9), 6391-6399.

72. Wan, Y.; Xu, J.; Lv, R. *Mater. Today* **2019,** *27*, 69-90.

73. Johnson, L. R.; Sridhar, S.; Zhang, L.; Fredrickson, K. D.; Raman, A. S.; Jang, J.; Leach, C.; Padmanabhan, A.; Price, C. C.; Frey, N. C. *ACS Catal.* **2019,** *10*(1), 253-264.

74. Zhao, T.; Zhang, S.; Guo, Y.; Wang, Q. *Nanoscale* **2016,** *8*(1), 233-242.

75. Tian, Y.-H.; Hu, S.; Sheng, X.; Duan, Y.; Jakowski, J.; Sumpter, B. G.; Huang, J. *J. Phys. Chem. Lett.* **2018,** *9*(3), 570-576.

76. Yang, T.; Tang, S.; Li, X.; Sharman, E.; Jiang, J.; Luo, Y. *J. Phys. Chem. C* **2018,** *122*(44), 25441-25446.

77. Huang, Y.; Wan, C. *J. Adv. Ceram.* **2020,** *9*, 271-291.

78. Azofra, L. M.; Sun, C.; Cavallo, L.; MacFarlane, D. R. *Chem. Eur. J.* **2017,** *23*(34), 8275-8279.

79. Zhao, J.; Zhao, J.; Cai, Q. *Phys. Chem. Chem. Phys.* **2018,** *20*(14), 9248-9255.

80. Zhang, L.; Ji, X.; Ren, X.; Ma, Y.; Shi, X.; Tian, Z.; Asiri, A. M.; Chen, L.; Tang, B.; Sun, X. *Adv. Mater.* **2018,** *30*(28), 1800191-1800197.

81. Zhao, J.; Chen, Z. *J. Am. Chem. Soc.* **2017,** *139*(36), 12480-12487.

82. Ling, C.; Niu, X.; Li, Q.; Du, A.; Wang. J. *J. Am. Chem. Soc.* **2018,** *140*(43), 14161-14168.

83. Chen, S.; Perathoner, S.; Ampelli, C.; Mebrahtu, C.; Su, D.; Centi, G. *Angew. Chem. Int. Ed.* **2017,** *56*(10), 2699-2703.

84. Xiaoyan, S.; Rui, W.; Dangsheng, S. *Chin. J. Catal.* **2013,** *34*(3), 508-523.

85. Fei, R.; Yang, L. *Nano Letters* **2014,** *14*(5), 2884-2889.

86. Kumar, C. V. S.; Subramanian, V. *Phys. Chem. Chem. Phys.* **2017,** *19*(23), 15377-15387.

87. Cheng, Y.; Song, Y.; Zhang, Y. *Phys. Chem. Chem. Phys.* **2019,** *21*(44), 24449-24457.

88. Qiu, W.; Xie, X.-Y.; Qiu, J.; Fang, W.-H.; Liang, R.; Ren, X.; Ji, X.; Cui, G.; Asiri, A. M.; Cui, G.; Tang, B.; Sun, X. *Nature Commun.* **2018,** *9*(1), 3485-3493.

89. Natali, F.; Ruck, B. J.; Trodahl, H. J. *U.S. Patent Application* 16/628,214, filed May 13, 2021.

90. Chan, J. R.; Lambie, S. G.; Trodahl, H. J.; Lefebvre, D.; Le Ster, M.; Shaib, A.; Natali, F. *Phys. Rev. Mater.*, **2020**, *4*(11), 115003-115008.

91. Xie, X. Y.; Xiao, P.; Fang, W. H.; Cui, G; Thiel, W. *ACS Catal.* **2019**, *9*(10), 9178-9187.

Alfred "Fred" Fischer

PhD (Cant.), FNIC, FCIC, FRSC, 1932-2021

Fred Fischer, who passed away on 10 December 2021, emerged from a West Coast gold mining family to become a notable scientist, mentor and administrator.

A childhood brush with polio sent young Fred from his rural home to convalesce at Loreto College in Christchurch, where his academic promise was so evident that he was kept on as a scholarship pupil. He was dux of St. Bede's College in 1949, winning a University of New Zealand national entrance scholarship.

At Canterbury University College, Fred was Senior Scholar in chemistry in his BSc graduating year, 1953. Upon completing his MSc with 1st class honours in 1955, he joined the chemistry department staff under the mentorship of Jack Vaughan. During the next few years he married, had two daughters and was promoted to Lecturer. In 1960 he completed his PhD in organic chemistry with a thesis entitled, "Polar effects of substituents on the acid- and base-catalysed enolisation of benzyl phenyl ketone".

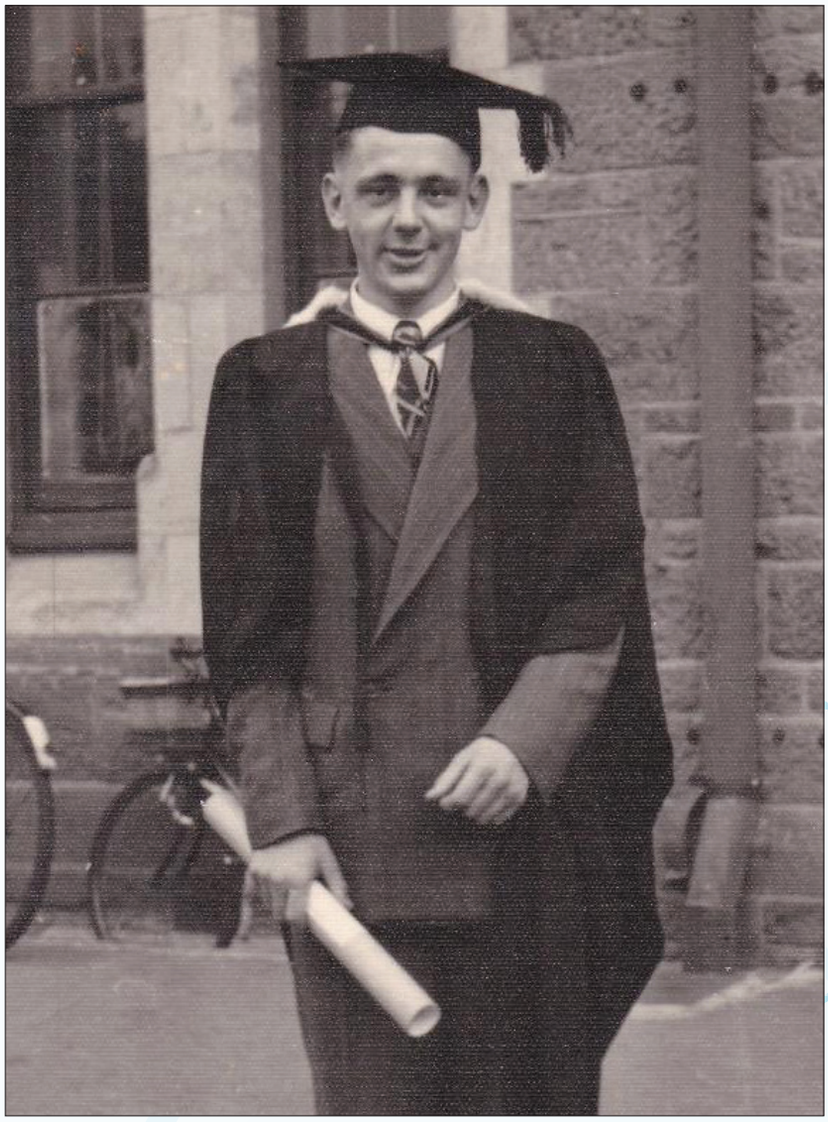

Fred Fischer in 1953

A post-doctoral research fellowship under George S. Hammond at the California Institute of Technology sent Fred and his young family to California in 1960. Not deterred by US/NZ double taxation, they subsisted on a shoestring and made the most of this American adventure. Son Martin was born in 1962 after returning to New Zealand.

Fred was Chair of the Canterbury branch of NZIC in 1965 and was promoted to Reader at UC in 1966.

A Nuffield Fellowship enabled a sabbatical year in 1966-67 at the University of Sussex, applying the new technology of mass spectrometry to the investigation of aromatic substitution reactions in benzene-type compounds.

Overseas opportunities beckoned and in January 1969, Fred joined the young University of Victoria in British Columbia, Canada as a full Professor of Chemistry. Fred's career at UVic quickly expanded to administrative roles, although he was noted for carving out time to maintain an active research laboratory. He sponsored overseas PhD students and promoted diversity in academia. He served as Acting Head of the Chemistry Department (1972-73), Dean of Arts & Science (1975-78), Vice-President, Academic (1979-83), Acting Dean of Engineering (1985-86) and Associate Vice-President, Administration (1989-95).

He redesigned the university pension plan with a life income fund type option that was subsequently adopted in provincial and federal legislation and is now in many other Canadian pension plans.

Retirement tributes from colleagues lauded Fred's industry, tact, objectivity, dedication, wisdom and mentorship. His CV listed 112 articles in refereed journals.

When Fred could tear himself away from the university, he was a blunt but tender-hearted family man, a lover of walks with family and friends, and a voracious reader who maintained life-long curiosity. He plunged into geological research and provided logistical support for his brother John's Yukon gold mining initiative in the 1990s.

After retirement, he and his wife Cathreen maintained their New Zealand connections with regular trips to visit family and friends. When advancing Alzheimer's disease forced Fred's move into long term care in late 2020 his bedrock warmth, humour and humility endeared him to staff and fellow residents.

Fred in 1997

Son Martin's death in 1984, of Hodgkin's lymphoma at the age of 22 years, was a great blow. Fred was also predeceased by wife Cathreen in 2020. He is survived by daughters Ann and Wendy in Canada, Ann's daughter Raphaella, a PhD student at Queen Mary University of London, Wendy's sons James and Alexander in Canada, brother John and nephews Mark and Brent in Greymouth and extended family throughout New Zealand and beyond.

Contributed by Ann Jackson.